



# Comprehensive Non-targeted Molecular Characterization of Organic Aerosols in the Amazon Rainforest

Denis Leppla<sup>1</sup> and Stefanie Hildmann<sup>1</sup>, Nora Zannoni<sup>2,a</sup>, Leslie Kremper<sup>2</sup>, Bruna Hollanda<sup>2,c</sup>, Jonathan Williams<sup>2,3</sup> Christopher Pöhlker<sup>2</sup>, Stefan Wolff<sup>2,b</sup>, Marta Sá<sup>4</sup>, Maria Christina Solci<sup>5</sup>, Ulrich Pöschl<sup>2</sup>, Thorsten Hoffmann<sup>1</sup>

<sup>1</sup>Chemistry Department, Johannes Gutenberg - University, Mainz, 55128, Germany

<sup>2</sup>Chemistry, Max Planck-Institute for Chemistry, Mainz, 55128, Germany

<sup>3</sup>Climate and Atmosphere Research Center, The Cyprus Institute, Nicosia, Cyprus

<sup>4</sup>Large-Scale Biosphere–Atmosphere Experiment in Amazonia (LBA), Instituto Nacional de Resquisas da Amazônia/INPA, Manaus, AM, Brazil

<sup>5</sup>Department of Chemistry Universidade Estadual de Londrina, Londrina, PR, Brazil

<sup>a</sup>now at: Institute of Atmospheric Sciences and Climate, National Research Council (CNR-ISAC), 40129 Bologna, Italy

<sup>b</sup>now at: German Weather Service, Offenbach am Main, 63067, Germany

<sup>c</sup>now at: Hessian Agency for Nature Conservation, Environment and Geology, Wiesbaden, Germany

Correspondence to: Thorsten Hoffmann (t.hoffmann@uni-mainz.de)

## Abstract

The Amazon rainforest plays a crucial role in the global climate system, hydrological cycle, and earth's energy balance. As one of the planet's least industrialized regions, it allows investigation of organic aerosol formation and constituents under almost pristine conditions. Nevertheless, human activities are known to affect this ecosystem – especially during the dry season. In this study, ambient aerosol samples collected at the Amazon Tall Tower Observatory (ATTO) during two dry and two wet seasons were characterized by high-resolution mass spectrometry (HR-MS). Comprehensive non-targeted data evaluation was applied to identify thousands of molecular formulae. Most were found to be associated with oxidation products of isoprene and monoterpenes, highlighting the predominance of biogenic secondary organic aerosols (SOA) at ATTO. The chemical composition exhibited distinct seasonal patterns with more processed organic compounds during the dry season, which can be explained by an increase of later-generation oxidation products due to reduced wet deposition and enhanced long-range transport. Mono- and polycyclic heteroaromatic components from biomass burning (BB) sources were enhanced during the dry seasons and the second wet season. The wet season was generally characterized by less oxidized compounds, associated with freshly formed SOA particles. Height-resolved measurements showed the forest canopy to be the main source for biogenic emissions with higher concentrations of early terpene oxidation products lower down. Overall, our results provide new insights into the molecular characteristics and seasonality of organic particulate matter at ATTO, helping to constrain the sources and interactions of aerosols, clouds, and precipitation in the Amazon rainforest.



## 1 Introduction

Organic particulate matter (PM) accounts for up to 90 % of the total atmospheric aerosol mass (Kanakidou et al., 2005; Kroll and Seinfeld, 2008; Jimenez et al., 2009). While primary organic aerosols (POA) are emitted directly into the atmosphere (e.g., combustion of biomass), secondary organic aerosols (SOA) are produced by oxidative processes and transformations of volatile organic compounds (VOC), followed by their nucleation and/or condensation in the atmosphere (Seinfeld and Pankow, 2003). Numerous studies have illustrated the complex chemical composition of organic aerosols covering various compound classes and thousands of different organic species (Tolocka et al., 2004; Zhang et al., 2007; Goldstein and Galbally, 2007; Wozniak et al., 2008; Nizkorodov et al., 2011). Organic aerosols have a substantial impact on climate and human health (Pöschl, 2005; Hallquist et al., 2009). Consequently, clarifying the chemical composition of organic aerosols is an essential task of atmospheric-related studies.

Compounds in OA feature a huge variety of functionalities, polarities, and volatilities at various concentration regimes (Goldstein and Galbally, 2007) which poses major challenges for analytical techniques (Nozière et al., 2015). Traditional gas chromatography and liquid chromatography systems coupled with mass spectrometry (GC/MS, LC/MS) have proven useful in identifying certain OA species (Hoffmann et al., 2011). However, these methods are limited to compounds with specific physicochemical properties and, thus, not adequate to resolve complex organic mixtures (Hildmann and Hoffmann, 2024). Hence, high-resolution mass spectrometry (HR-MS) with enhanced resolving power ( $\geq 100\,000$ ) and high mass accuracy ( $\leq 5$  ppm) has received more and more attention in atmospheric aerosol research (Nozière et al., 2015; Burgay et al., 2023; Xie and Laskin, 2024). The combination with soft ionization methods, such as electrospray ionization (ESI), allows a detailed characterization of complex OA samples (Nizkorodov et al., 2011). Several studies have already proven the potential of HR-MS in smog chamber experiments (Thoma et al., 2022; Frauenheim et al., 2024). Hundreds of different organic species have been detected in SOA samples generated by isoprene and monoterpene oxidation (Tolocka et al., 2004; Bateman et al., 2008; Nguyen et al., 2010). Additionally, OA samples from urban and pristine environments have been analyzed by HR-MS to identify transformation processes and potential sources of aerosol constituents (Wang et al., 2017; Tong et al., 2016; Kourtchev et al., 2013; Hettiyadura et al., 2021; Lin et al., 2018).

The Amazon basin is one of the most pristine ecosystems on Earth, comprising approximately 40% of all tropical forests (Goulding and Barthem, 2003; Baccini et al., 2012). The ecosystem impacts the earth's climate through its role in the hydrological cycle, its role as storage for atmospheric carbon, and the radiative effects of its associated cloud systems. However, the Amazon region is heavily impacted by anthropogenic activities such as deforestation (Andreae et al., 2015). Observations and modeling studies show that climate change and deforestation affect the carbon and hydrological cycles in Amazonia changing to carbon neutrality and affecting precipitation downwind (Artaxo et al., 2022). Consequently, significant seasonal fluctuations in OA concentrations are observed, influencing the radiation balance and cloud processing (Pöhlker et al., 2023; Pöschl et al., 2010; Artaxo et al., 2013). Despite the Amazon's pivotal role in the Earth's atmosphere, our comprehension of the underlying atmospheric processes remains incomplete. For instance, the role of organic compounds in nucleation, cloud formation processes, or the aging and processing of aerosol components remains unresolved. An understanding of these processes is a fundamental prerequisite for assessing the future of the ecosystem in the context of climate and land use change (Shrivastava et al., 2019). To address such questions, a molecular characterization of organic aerosol in the Amazon rainforest is required.

In this study, LC-HR-MS was used to analyze aerosol filter samples from the Amazon rainforest covering several seasons from 2018 and 2019. Sophisticated non-targeted analytical techniques were applied to link the OA molecular composition with meteorological conditions, potential emission sources, and (trans)formation processes. The work provides a comprehensive molecular-level understanding of organic aerosols in the Amazon rainforest, a key region for studying interactions between natural and anthropogenic influences on the atmosphere. The Amazon's organic aerosols play a critical



role in regional and global climate regulation, biogeochemical cycles, and cloud formation processes. Despite their significance, the molecular complexity and variability of these aerosols remain underexplored. By employing advanced non-targeted analytical approaches, this study aims to fill knowledge gaps regarding their sources, transformations, and impacts, ultimately contributing to improved models of atmospheric chemistry and climate dynamics.

## 2 Experimental section

### 2.1 Aerosol sampling

Ambient PM<sub>2.5</sub> aerosol samples were collected in the Amazon rainforest at the Amazon Tall Tower Observatory (ATTO). In total, four measurement campaigns were performed to investigate seasonal variations of the SOA chemical composition. The sampling time covered the wet season 2018 (14/Apr/2018 – 19/Apr/2018), the dry season 2018 (22/Oct/2018 – 31/Oct/2018), the wet season 2019 (04/Mar/2019 – 14/Mar/2019), and the dry season 2019 (20/Sep/2019 – 26/Sep/2019). The research site allows height-resolved measurements on a 325 m tall tower in the central Amazon basin (coordinates: S 02°08.752' W 59°00.335') and is described in detail by Andreae et al. (2015). Shortly, the nearest urban region is Manaus which is located approximately 150 km southwest of ATTO. The station is part of the Uatumã Sustainable Development Reserve (UDSR) and is reached via the roughly 12 km distant Uatumã river. The tower is located at about 120 m above sea level on a plateau that is embedded in a dense, non-flooded forest (terra firme) with adjacent floodplain forests and white-sand soil savannas (campinas) and forests (campinaranas). The area at ATTO is characterized by a canopy height of about 35 m. The meteorological conditions at ATTO depend on the location of the Intertropical Convergence Zone (ITCZ) providing clean and rainy circumstances from February until May and polluted and drier conditions from August to November with strong contributions from anthropogenic deforestation and land-use change (Pöhlker et al., 2019). Relevant meteorological parameters were constantly measured and are shown in the supporting information. The corresponding wind profiles and backward trajectories were generated by the HYSPLIT Trajectory Model (Stein et al., 2015; Rolph et al., 2017).

Ambient PM<sub>2.5</sub> filter samples were collected at three different heights at the tower (wet season 2018: 42 m, 150 m, 320 m; dry season 2018 and wet season 2019: 80 m, 150 m, 320 m; dry season 2019: 0 m, 80 m, 320 m) using borosilicate glass microfiber filter bonded with PTFE (Pallflex® Emfab, 70 mm diameter). A pre-separator (Digitel, DPM2.3) was set up in front of the filter to only collect the size fraction with aerodynamic particle diameters below 2.5 µm at constant flow rates of 38 L min<sup>-1</sup>. The sampling duration was set to 10 h – 14 h to allow daytime and nighttime related sample collection while ensuring sufficient particle mass on the filter material. Blank filters were collected according to the mentioned procedures but with disabled pumps. In total, 246 filter samples were collected and stored in the freezer at -18 °C before their analysis.

### 2.2 Sample preparation and analysis

One half of each filter sample was extracted three times by adding 1.5 mL of a 9:1 mixture of methanol and water (Fisher Scientific, Optima™ grade). The samples were subsequently agitated for 30 min on a laboratory shaker. The combined liquid phases were filtered afterward through a 0.2 µm PTFE syringe filter (Carl Roth, Rotilabo® KC 94.1) and evaporated completely by a gentle stream of N<sub>2</sub>. The residue was then reconstituted in 700 µL of a 9:1 mixture of water and acetonitrile (Fisher Scientific, Optima™ grade).

Ten microliters of each sample were analyzed three times by ultra high-performance liquid chromatography (UHPLC) (ThermoFisher Scientific, UltiMate 3000) coupled to a high-resolution Orbitrap mass spectrometer (MS) (ThermoFisher Scientific, Q Exactive™). A heated electrospray ionization (ESI) source was installed and operated in the negative ionization mode. The instrument was externally calibrated with a calibration solution (Fisher Scientific, Pierce™) and a 2 mM sodium acetate aqueous solution providing mass accuracies below 1 ppm. The sample analysis was performed in the range of *m/z* 50 – 750 at a mass resolving power of 140 000 at *m/z* 200. The following ESI-MS parameters were used for the measurements: ESI capillary temperature 300 °C; spray voltage -3.2 kV; sheath gas flow 30; auxiliary gas flow 10, S-lens



125 RF level 50%. The UHPLC system was operated with a HSS T3 column (100 × 2.1 mm ID, 1.8 μm, Waters, ACQUITY UPLC®) and the mobile phase A (water with 2% acetonitrile and 0.04% formic acid) and mobile phase B (acetonitrile with 2% water). The conditions for gradient elution were as follows: 0 – 2 min 0% B, 2 – 9 min linear increase to 30% B, 9 – 15 min linear increase to 95% B, 15 – 17.5 min 95% B, 17.5 – 19 min linear decrease to 0% B, 19 – 21 min 0% B at a constant flow rate of 350 μL min<sup>-1</sup>.

### 130 2.3 Non-Targeted Data Evaluation

The LC/MS data were processed by MzMine 2.30 to obtain molecular formulae C<sub>c</sub>H<sub>h</sub>O<sub>o</sub>N<sub>n</sub>S<sub>s</sub> with the following limitations: 2 ≤ C ≤ 40, 2 ≤ H ≤ 100, 0 ≤ O ≤ 40, 0 ≤ N ≤ 4, 0 ≤ S ≤ 2. Fluorine was not taken into account in the data evaluation, although recent studies show that fluorine compounds in the form of per- and polyfluoroalkyl substances (PFAS) can also be detected in traces in aerosols over tropical rainforests (Kourtchev et al., 2024). The mass tolerance for the formula assignment was set to ± 2 ppm considering isotope patterns. Adducts were removed and only ions present in all three repeated measurements were retained. The signal intensities per sample were averaged afterward. Blank samples were processed accordingly and subtracted. Only compounds with signal-to-background ratios ≥ 3 were kept for further evaluations. The number of rings and double bonds was described by the double bond equivalent (DBE) for each assigned formula providing information on the degree of unsaturation and calculated by equation (2.1) (Badertscher et al., 2001):

$$140 \quad DBE = nc - \frac{n_H}{2} + \frac{n_N}{2} + \frac{n_S}{2} + 1 \quad (2.1)$$

where *n* describes the number of the respective element.

Based on the DBE values the aromaticity equivalent (Xc) was calculated by equation (2.2) to identify mono- and polycyclic aromatic compounds (Yassine et al. (2014)):

$$145 \quad Xc = \frac{3(DBE - (p \cdot n_o + q \cdot n_s)) - 2}{DBE - (p \cdot n_o + q \cdot n_s)} \quad (2.2)$$

where *p* and *q* represent the fraction of oxygen and sulfur atoms that are involved in the π-bond structure of the molecule. Consequently, these values can vary according to different compound classes. While *p* = *q* = 0.5 is suggested for carboxylic acids, esters, and nitro functional groups, *p* and *q* are set to either 0 or 1 for aldehydes, ketones, alcohols, ethers, and nitroso classes. In the present study, *p* = *q* = 0.5 was used to calculate Xc considering that negative ESI analysis is highly sensitive to carboxylic acids (Kourtchev et al., 2016; Wang et al., 2017). According to Yassine et al. (2014), Xc ≥ 2.50 and Xc ≥ 2.71 are indicating monocyclic and polycyclic aromatic compounds, respectively.

155 The carbon oxidation state (OSC) for CHO compounds was calculated following the simplified equation (2.3) (Kroll et al. (2011)):

$$OSC \approx 2 \cdot \frac{n_o}{n_c} - \frac{n_H}{n_c} \quad (2.3)$$



with the elemental ratios  $O/C$  and  $H/C$ , respectively.

Furthermore, the saturation vapor pressure ( $C^0$ ) has been calculated to predict the volatility of OA compounds according to equation (2.4) Donahue et al. (2011) and Li et al. (2016):

$$\log_{10} C^0 = (n_C^0 - n_C) \cdot b_C - n_O b_O - 2 \cdot \frac{n_C n_O}{n_C + n_O} \cdot b_{CO} - n_N b_N - n_S b_S \quad (2.4)$$

where  $n_C^0$  describes the reference carbon number,  $b$  represents the contribution of each element to  $\log_{10} C^0$ , and  $b_{CO}$  denotes the carbon-oxygen nonideality. The  $C^0$  values have been calculated for compound classes containing C, H, O, N, and S atoms. The parameters for the calculation based on Li et al. (2016) are listed in the supporting information Table S 1.

Kendrick mass (KM) analysis was used to assign homologous series of the detected compounds, which vary only in the number of a defined base unit (Kendrick, 1963; Hughey et al., 2001). In the present study,  $CH_2$  was chosen as the base unit by rescaling the exact mass of 14.01565 to 14.00000.  $KM_{CH_2}$  was calculated according to equation (2.5) for each compound by renormalizing the exact mass scale (Hughey et al., 2001):

$$KM_{CH_2} = \text{exact mass} \cdot \left( \frac{14.00000}{14.01565} \right) \quad (2.5)$$

Subsequently, the Kendrick mass defect (KMD) was calculated by equation (2.6):

$$KMD_{CH_2} = \text{nominal KM} - KM_{CH_2} \quad (2.6)$$

where *nominal KM* describes the KM rounded to the next integer. Consequently, compounds differing only in their number of  $CH_2$  units have the same KMD values. Homologous series can be identified as horizontal lines in KMD plots.

### 3 Results and Discussion

The chemical complexity of the OA samples is highly influenced by stochastic regional events and the respective meteorological conditions between sampling days, such as the height of the mixing layer and the wind direction. In order to take these influences into account, a distinction is made in the present study between background, variable and total organic aerosol compounds. Only compounds that were observed in more than 75 % of all samples were defined as background compounds. They presumably describe the local OA characteristics, as it is assumed that they are not dependent on individual emission events. For the variable OA characteristics, the evaluation was carried out by subtracting the previously determined background compounds from the total number of identified compounds (= background compounds + variable compounds). The remaining compounds are attributed to irregular atmospheric events, presumably caused by different meteorological conditions. Compounds that were only detected once in the respective data set were excluded as they were not considered representative.

#### 3.1 Total OA characteristics

All detected compounds were separated by reversed-phase HPLC prior to MS analysis, which increases the number of measurable compounds and reduces the risk of ion suppression in the ESI source. The chemical composition of the SOA



samples was mainly influenced by seasonal effects during the measurement campaigns. Molecular weights (MW) in the range below 250 Da could be assigned to the majority of observed substances in both seasons, while the aerosol composition in the dry season additionally showed signals in the oligomeric range between 300 and 450 Da with lower intensity. While several studies have shown that ozonolysis of biogenic VOCs (e.g.  $\alpha$ -pinene,  $\beta$ -pinene, isoprene) in smog chamber experiments produces compounds with high molecular weight and increased signal intensities in the oligomeric range (Kourtechev et al., 2014a; Reinhardt et al., 2007), ions above 450 Da contributed insignificantly to the total number of compounds in the present filter samples.

All filter samples reveal a high chemical diversity with 875 – 1940 unambiguously assigned molecular formulae with a large fraction of isomeric compounds (69% – 85%) (Table I), highlighting the importance of pre-separating the samples by HPLC.

The identified molecular formulae were divided into four subgroups according to their elemental composition: CHO, CHON, CHONS, and CHOS. The CHO subgroup is predominant with  $(56 \pm 6)$  % in all samples, followed by CHON with  $(20 \pm 7)$  %, CHOS  $(17 \pm 5)$  %, and CHONS  $(7 \pm 1)$  %, although the contribution of sulfur- and/or nitrogen-containing compounds increases at higher MWs. This trend is in good agreement with similar studies from remote environments (e.g. Amazonia, Brazil, Kourtechev et al., 2016; Hyytiälä, Finland, Kourtechev et al., 2013), while studies from a suburban and urban environment revealed enhanced contributions of CHON and CHONS compounds (Pearl River Delta region, China, Lin et al., 2012; Cambridge, UK, Rincón et al., 2012; Shanghai, China, Wang et al., 2017), proving an increased relevance of nitrogen and sulfur chemistry in more polluted areas. The total calculated elemental ratios are highly variable throughout the seasonal measurement campaigns with  $0.60 \pm 0.37$  (mean value  $\pm$  standard deviation of the data set) and  $1.47 \pm 0.49$  for O/C and H/C during the dry season and  $0.49 \pm 0.32$  and  $1.56 \pm 0.45$  during the wet season, respectively. The wide variability indicates a high chemical complexity within the data set. Comparable values were reported from the boreal forest in Hyytiälä, Finland ( $0.58$  and  $1.54$  for O/C and H/C, respectively) (Kourtechev et al., 2013). Additionally, the elemental ratios obtained in this study are consistent with smog chamber experiments using certain biogenic VOCs for SOA generation, e.g.  $\alpha$ -pinene ( $0.42$  –  $0.55$  for O/C and  $1.5$  for H/C, Putman et al., 2012) and limonene ( $0.5$  –  $0.6$  for O/C and  $1.5$  –  $1.6$  for H/C, Kundu et al., 2012). Vertical profiles of  $\alpha$ -pinene and limonene were measured at ATTO showing different chemical speciations between day and night (Zannoni et al., 2020; Yáñez-Serrano., 2018). The averaged total oxidation states of CHO compounds in the wet seasons ( $-0.681 \leq \text{OSC} \leq -0.486$ ) are lower than in the dry seasons ( $-0.525 \leq \text{OSC} \leq -0.324$ ) indicating more processed organic aerosol in the dry seasons than in the wet seasons. Furthermore, the averaged total aromaticity indices ( $\text{Xc} \leq 2.50$ ) do not suggest a significant portion of mono- or polycyclic hydrocarbons.

**Table I: Summary of all observed MS signals with unambiguous molecular formula assignment for the four measurement campaigns in 2018 and 2019 (wet season = WS, dry season = DS). The signals are divided into four subgroups regarding their elemental composition. Additionally, the average values<sup>1</sup> of molecular weight (MW), carbon oxidation state (OSC), aromaticity index (Xc), and isomeric fraction are listed.**

Season	Height m	Signals	CHO %	CHON %	CHONS %	CHOS %	MW Da	OSC <sup>2</sup>	Xc	Isomers %
WS18	42	1095	54	30	6	10	271	-0.647	0.872	77
	150	875	67	15	7	11	261	-0.606	0.977	80
	320	1293	43	41	7	9	293	-0.681	0.822	70
DS18	80	1856	51	19	7	23	245	-0.324	1.050	83
	150	1940	51	18	8	23	240	-0.353	1.051	85
	320	1720	52	18	8	22	245	-0.330	1.070	84



	80	1555	55	19	5	21	250	-0.535	0.907	81
<b>WS19</b>	150	1081	57	18	7	18	252	-0.486	0.922	81
	320	1287	62	17	6	15	255	-0.558	1.017	82
	0	1328	60	17	5	18	237	-0.425	0.831	69
<b>DS19</b>	80	1225	61	14	6	19	233	-0.439	0.906	84
	320	1050	62	15	6	17	246	-0.525	0.975	77

<sup>1</sup> Average values are calculated based on the molecular composition of each compound.

<sup>2</sup> Only CHO compounds are considered in the calculation of OSC.

## 230 3.2 Background OA characteristics

A clear seasonality characterizes the molecular background composition of organic aerosols at ATTO. Air masses at ATTO are in response to the annual north-south migration of the ITCZ (Intertropical Convergence Zone) leading to a seasonal alternation between north-easterly winds during the wet seasons and south-easterly winds during the dry seasons (Pöhlker et al. 2019). Seven-day HYSPLIT backward trajectories (Stein et al., 2015) show that air masses need approximately 6 – 7 days from the west coast of Africa to pass the Atlantic Ocean towards ATTO (see Figure S 2, Figure S 3). Higher wind speeds of up to 15 – 20 m s<sup>-1</sup> were observed during the wet seasons (dry seasons 10-15 m s<sup>-1</sup>), leading to a dilution of the particle phase at ATTO (Figure S 1). Comparable to cleaner marine air masses from the ocean, lower background signals are detected during the wet seasons. In contrast, the dry seasons are considerably influenced by biomass burning (Table S 3) and other anthropogenic emissions from the eastern regions in Brazil (Artaxo, 2002; Andreae et al., 2015), resulting in higher concentrations of particulate matter (PM) (Figure S 4, Figure S 5). Concentrations up to 15 µg m<sup>-3</sup> have been observed during the dry periods while approximately ten times lower concentrations were detected during the wet season.

The chemical composition of background OA also reflects these seasonal changes in meteorological conditions. 72 – 215 organic compounds were detected during the dry seasons, while 28-60 different compounds were observed during the wet seasons (Table S 2). The molecular formulae in the wet seasons are predominated by the CHO subgroup (90 ± 7) %, followed by CHOS with (8 ± 7) %, CHONS (1 ± 1) %, and CHON (1 ± 2) %. The dry seasons show a comparable predominance of the CHO subgroup (93 ± 3) % and CHONS compounds (1 ± 1) % but an increased fraction of CHON compounds (4 ± 1) % and a decreased fraction of CHOS compounds (3 ± 2) %. Furthermore, the averaged background aromaticity indices ( $X_c \leq 2.50$ ) do not suggest a significant portion of mono- or polycyclic hydrocarbons in both seasons.

### 3.2.1 Van-Krevelen diagrams

Van Krevelen diagrams (VK diagrams) are used to visualize similarities and differences, e.g. between measuring locations, measuring heights, daily or seasonal influences. In a VK diagram, the H/C ratio is shown as a function of the O/C ratio for each molecular formula detected in a sample. This helps for example to visualize the degree of oxidation of the particle phase organics as the most oxidized molecules are located at the lower right corner (Zhang et al., 2021). Consequently, the most saturated and reduced species are found in the upper left region. VK diagrams of the wet and dry season 2018 at different sampling heights are shown in Figure 1. The corresponding VK diagrams for the wet and dry season 2019 show very similar patterns and can be found in Figure S 7. The signal intensity is proportional to the size of the symbols. However, the signal intensities of the various compounds certainly only provide semi-quantitative results and should therefore only be converted into concentrations to a limited extent, as different substances are detected with different sensitivities due to the selectivity of





the electrospray ionization with regard to ion yield. The most intense ion signals are summarized in Table II with their molecular formula, their possible identity and the precursor species.

**General.** The background compounds in the wet seasons are all non-aromatics with a high O/C-ratio ( $O/C \geq 0.5$ ) and either C4-5 or C7-8 backbones, probably resulting from isoprene and monoterpene (mainly  $\alpha$ -pinene,  $\beta$ -pinene, and limonene) oxidation (Kleindienst et al., 2007; Nguyen et al., 2010; Worton et al., 2013; Hammes et al., 2019). These precursor compounds are the most prevalent biogenic VOCs in the Amazon rainforest, released by a large diversity of terrestrial vegetation (Guenther et al., 1995; Greenberg et al., 2004; Zannoni et al., 2020). The more complex chemical background of the dry seasons is clearly illustrated in the VK diagram in Figure 1. Especially the dry season 2018 was characterized by a high abundance of signals with H/C ratios  $\geq 1.5$  and O/C ratios  $\leq 0.5$ . These compounds are commonly attributed to aliphatic species, which can be related to both, biogenic and anthropogenic sources. Simultaneously, several compounds with low elemental ratios ( $H/C \leq 1.0$  and  $O/C \leq 0.5$ ) were identified as background compounds, typically associated with aromatic hydrocarbons (Wozniak et al., 2008; Mazzoleni et al., 2012). Species within this region were exclusively observed during the dry season 2018, where the highest particle concentrations were detected.

**Isoprene SOA.** The ion at  $m/z$  149.0455 ( $C_5H_{10}O_5$ ) was observed in all analyzed filter samples with high intensities. This component has been detected in isoprene oxidation chamber experiments and field studies using SOA filter sampling (Krechmer et al., 2015; Chen et al., 2020).  $C_5H_{10}O_5$  was identified to be the most dominant species produced during the photooxidation of isoprene hydroxy hydroperoxides (ISOPOOH), which are important products of the isoprene oxidation under low-NO conditions (Krechmer et al., 2015; Paulot et al., 2009; Nagori et al., 2019). OH- initiated oxidation of ISOPOOH leads to only 2.5% to organic aerosols including  $C_5H_{10}O_5$ , while approximately 90% result in the formation of isoprene epoxydiol (IEPOX) and other gas-phase products (Krechmer et al., 2015). However,  $C_5H_{10}O_5$  was also observed during isoprene ozonolysis and during isoprene photooxidation under high-NO conditions (Jaoui et al., 2019). Consequently, the latter pathways appear to be the dominant reactions during the dry seasons with increased NO concentrations (Figure S 6), while the ISOPOOH-SOA pathway under low-NO conditions is presumed during the wet seasons.

**IEPOX-OS.** The samples from the 2018 wet season showed the ion at  $m/z$  215.0231 ( $C_5H_{12}O_7S$ ) as the most intense signal related to IEPOX-derived organosulfates (OS) (Surratt et al., 2007; Surratt et al., 2008). It is established that these OSs are formed from the reactive uptake of IEPOX on acidic sulfate particles under low-NO conditions, which is in agreement with our findings. IEPOX-OS was also found on filter samples from the Amazon rainforest in another study (Kourtchev et al., 2016). The authors observed the highest intensities on filters highly affected by surrounding forest fires. Interestingly, the lowest number of active fires was recorded during the wet season 2018 campaign (Table S 3) (INPE - Instituto Nacional de Pesquisas Espaciais, 2020). Sulfate concentrations during the wet seasons are mainly attributed to biogenic and marine sources (Andreae et al., 2015), while increased levels during drier seasons are related to combustion activities (Pöhlker et al., 2018). Sulfur compounds can also be emitted from soils showing higher emissions with higher soil moisture (Pugliese et al., 2023) leading to a significant organosulfur source from the forest itself. This suggests that IEPOX-OS is a relevant SOA constituent, regardless of the current season, and is consistent with the idea of mixed anthropogenic and biogenic sources.

**Monoterpene SOA.** The wet season campaigns were characterized by intense ion signals at  $m/z$  157.0506 ( $C_7H_{10}O_4$ ) and  $m/z$  171.0662 ( $C_8H_{12}O_4$ ), attributed to limonene and  $\alpha$ -pinene oxidation products, among others (Hammes et al., 2019; Eddingsaas et al., 2012; Thoma et al., 2022; Florou et al., 2024), suggesting that biogenic sources are the main contributor to SOA loading at ATTO. Furthermore, the intensities of  $\alpha$ -pinene oxidation products were higher in the dry than in the wet seasons.

**Aromatics.** All detected ions were classified by their aromaticity equivalent  $X_c$  according to Yassine et al. (2014), in order to identify mono- and polycyclic aromatic species. While monocyclic structures such as benzene and functionalized derivatives are indicated by values of  $X_c \geq 2.50$ , condensed polycyclic aromatic compounds are described by  $X_c \geq 2.71$ . Naphthalene is the smallest polycyclic structure meeting this criterion (Yassine et al., 2014; Wang et al., 2017). The dry season





campaigns were accompanied by an increased number of active fires and biomass burning (Table S 3). Consequently, the detected aromatic hydrocarbons are mainly attributed to anthropogenic sources (Henze et al., 2008).

**Hydrocarbons:** The dry season 2018 was characterized by the occurrence of several aromatic species with Xc values  $\geq 2.50$  (Figure S 8). The most intense signals correspond to the ions at  $m/z$  149.0243 ( $C_8H_6O_3$ ),  $m/z$  164.0353 ( $C_8H_7NO_3$ ),  $m/z$  193.0505 ( $C_{10}H_{10}O_4$ ), and  $m/z$  207.0298 ( $C_{10}H_8O_5$ ), each with DBE values  $\geq 6$ . These compounds were already identified as relevant components of biomass burning activities.  $C_8H_6O_3$  and  $C_{10}H_8O_5$  were observed during naphthalene photooxidation experiments in a chamber study (Kautzman et al., 2010; Chhabra et al., 2015; Thoma et al., 2022). Naphthalene and other polycyclic aromatic hydrocarbons (PAH) have been related to wood combustion processes in the literature and are considered to impact human health (Schauer et al., 2001; Chan et al., 2009; Samburova et al., 2016; Baumann et al., 2023).  $C_{10}H_{10}O_4$  might be a product formed during the degradation of cellulose and lignin, two important biopolymers (Kong et al., 2021). The  $MS^2$  spectrum (Figure S 9) revealed two fragments,  $CO_2$  and  $C_3H_4O_2$  (acrylic acid), leading to a tentative structure of ferulic acid.

**Nitro-hydrocarbons:**  $C_8H_7NO_3$  was assigned to a nitro-phenolic structure, which can be formed during biomass pyrolysis. This compound class is a major contributor to brown carbon (BrC) (Lin et al., 2016) and has been detected earlier in SOA samples from the Amazon rainforest (Claeys et al., 2012). The ion appeared in almost every sample of the dry season 2019 in high intensities, suggesting this compound to be an important biomass burning marker in this study. Another intense background ion was 4-nitrocatechol at  $m/z$  154.0146 ( $C_6H_5NO_4$ ), which has been previously considered as a marker compound for biomass burning OA (Iinuma et al., 2010; Claeys et al., 2012; Kourtchev et al., 2016).

**Polycycles:** The ion at  $m/z$  219.0455 ( $C_{15}H_8O_2$ ) appeared in the dry season 2019 samples and has already been reported in another study (Bruns et al., 2015). The authors identified this compound as an oxygenated PAH produced during wood combustion with a pyrene core structure, which seems reasonable according to the increased Xc Value of 2.82 and 12 DBE.

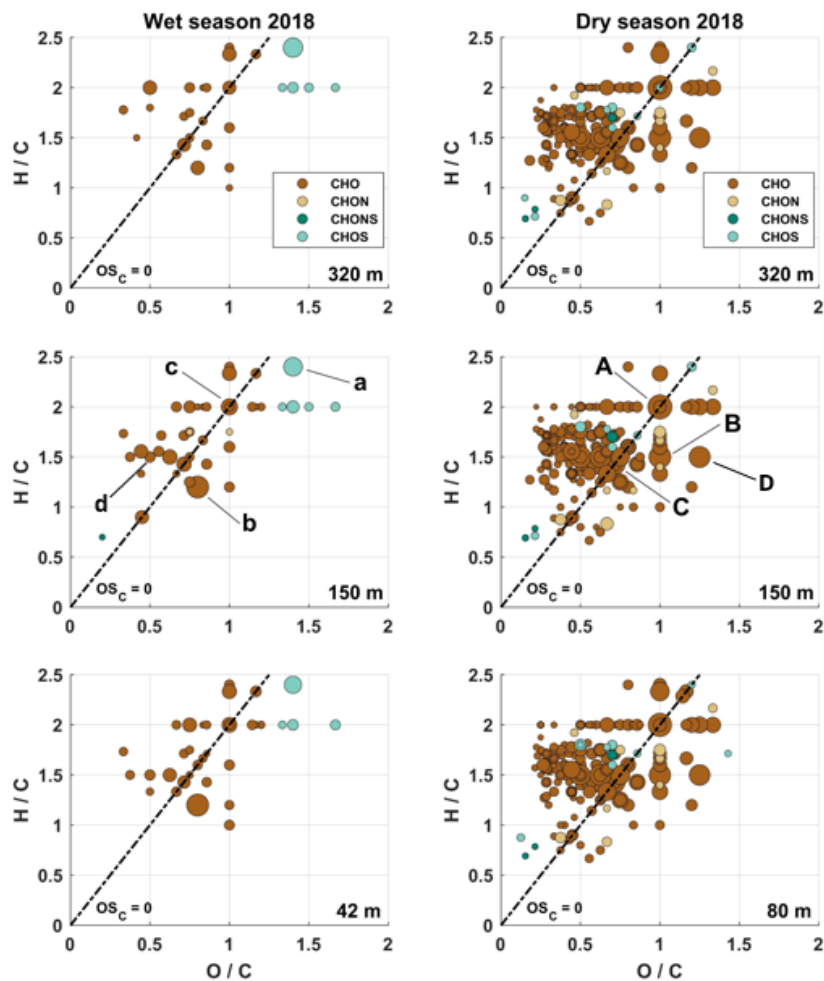


Figure 1: Van Krevelen plots from the wet season 2018 (left panel; sampling heights: 320 m, 150 m, 42 m) and the dry season 2018 (right panel; sampling heights: 320 m, 150 m, 80 m). Included are only molecular formulae that were present in more than 75% of the samples, respectively. The size of the data points represents the signal intensity of the corresponding peak. The four subgroups are distinguished with different colors. Compounds located on the black dashed line have an average carbon oxidation state of 0 (OSC = 0). The labels a-d and A-D correspond to the most intense signals further characterized in Table II.

Table II: Possible identities and precursors for the most intense signals from the background ions for the different seasons.

Season	ID <sup>1</sup>	Formula	<i>m/z</i>	OSC	Possible identity	Precursor	Reference
WS18	a	C <sub>5</sub> H <sub>12</sub> O <sub>7</sub> S	215.0231	-	IEPOX-OS	Isoprene	(Worton et al., 2013) (Kourtchev et al., 2016)
	b	C <sub>5</sub> H <sub>6</sub> O <sub>4</sub>	129.0194	0.4	Dicarboxylic acid / Peroxy acid	Methylfuran	(Joo et al., 2019)
	c	C <sub>5</sub> H <sub>10</sub> O <sub>5</sub>	149.0455	0.0	Carbonyl-tetrol / Epoxyl-tetrol / Carboxyl-triol	Isoprene	(Krechmer et al., 2015) (Chen et al., 2020)



	d	C <sub>8</sub> H <sub>12</sub> O <sub>4</sub>	171.0662	-0.5	Ketolimononic acid / Terpenylic acid	Limonene / $\alpha$ - pinene	(Hammes et al., 2019) (Eddingsaas et al., 2012)
<b>DS18</b>	A	C <sub>5</sub> H <sub>10</sub> O <sub>5</sub>	149.0455	0.0		See ID c	
	B	C <sub>4</sub> H <sub>6</sub> O <sub>4</sub>	117.0193	0.5	Succinic acid	-	(Wang et al., 2017)
	C	C <sub>7</sub> H <sub>10</sub> O <sub>5</sub>	173.0454	0.0		$\alpha$ -pinene	(Chen et al., 2020) (Kleindienst et al., 2007)
	D	C <sub>4</sub> H <sub>6</sub> O <sub>5</sub>	133.0142	1.0	Malic acid	Isoprene	(Nguyen et al., 2010)
<sup>1</sup> IDs correspond to the labels illustrated in Figure 1.							

### 3.2.2 Carbon oxidation states

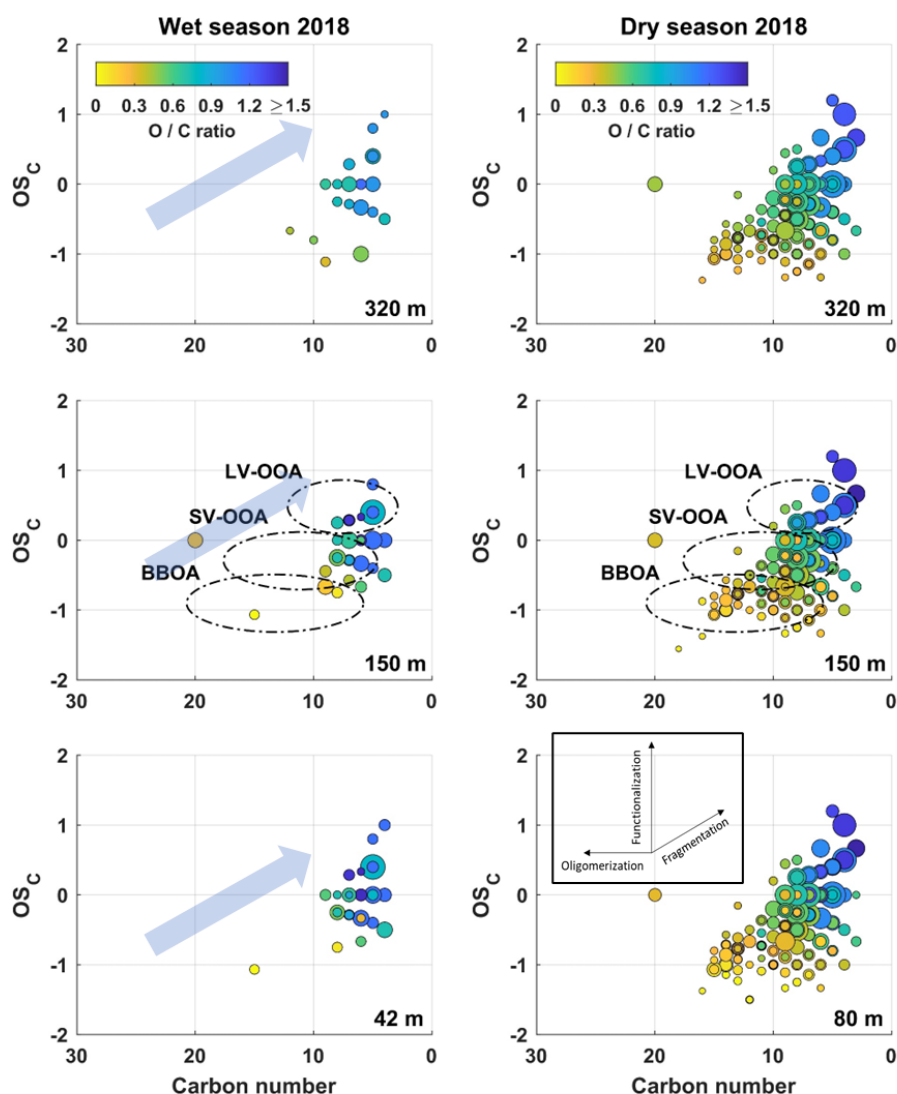
To further characterize the background chemical composition of the aerosol, the average carbon oxidation state (OSC) was calculated for each detected molecular CHO formula. This metric was introduced by Kroll et al. (2011) and is a useful parameter to describe complex mixtures of organic aerosols. Various chemical and physicochemical processes in the atmosphere are determined by the oxidation state of the organic components. For example, highly oxidized molecules (HOM) with sufficiently low volatility can form nuclei, which leads to the formation of new particles and subsequent particle growth, even of small particles (Bianchi et al., 2016; Molteni et al., 2016).

To give an impression of the position of the corresponding OSC values within the regular Van Krevelen plots, organic compounds with OSC = 0 are indicated by the dashed line in Fig. 1. To the left are compounds with an OSC < 0 (not or less oxidized), to the right are compounds with OSC values > 0, e.g. the HOMs, which are defined as molecules with O/C  $\geq$  0.6 and/or OSC  $\geq$  0 (Tu et al., 2016). As shown in Fig. 1, the samples from the 2018 dry season had the highest number of highly oxidized compounds, which accounted for about 30 % of the total number of compounds. The average molecular formula for the HOMs in the 2018 dry season was C<sub>6.5</sub>H<sub>8.6</sub>O<sub>5.1</sub> with C<sub>4</sub>-C<sub>10</sub> backbones, which can be interpreted that isoprene and monoterpene precursors are also the main source of HOMs in the Amazon rainforest in the dry season. The 2019 dry season showed fewer oxidized molecules, with a mean molecular formula of C<sub>6.7</sub>H<sub>10.2</sub>O<sub>5.7</sub>. However, it should be noted that the analysis of highly oxygenated compounds would benefit from the use of a more polar stationary phase of the LC column, as a more comprehensive analysis of analytes of the entire polarity range would be enabled. This would ensure that even the very polar species are not underestimated due to insufficient separation.

Figure 2 shows the OSC values as a function of carbon number for each CHO compound, with OSC values ranging from -1.5 to +1.2 in the dry seasons and from -1.1 to +1.0 in the wet seasons. This result is consistent with other studies in remote continental areas (Kourtev et al., 2013; Kourtev et al., 2016). Molecules with an OSC between -0.5 and -1.5 and a carbon number greater than seven are considered biomass-burning organic aerosol (BBOA). The comparison between dry and wet seasons clearly shows the large number of compounds associated with BBOA and that these substances contribute substantially to the SOA load of the Amazon rainforest during dry seasons. Interestingly, the contribution of BBOA-related compounds was significantly higher in the 2019 wet season (Figure S 10), which is likely due to the increased number of active fires during this period. In contrast, molecules with an OSC between -0.5 and +1.0 and less than 13 carbon atoms are generally associated with semivolatile and low-volatility oxygenated organic aerosol (SV-OOA and LW-OOA) (Kroll et al., 2011; Wang et al., 2017). These compounds are formed by multiple oxidation reactions and are commonly attributed to fresh and aged SOA,



360 respectively (Zhang et al., 2007; Jimenez et al., 2009). The background chemical composition during the dry seasons also revealed numerous compounds attributed to LV-OOA indicating more aged SOA components compared to the wet seasons. Whether the lower precipitation in the dry season and the associated longer residence times of the OA in the atmosphere are the cause of these observations, or whether these compounds also have their source in biomass combustion processes, cannot be clearly determined here. In contrast, the majority of background compounds during rainy seasons are associated with SV-OOA, suggesting that local biogenic emissions are the main source of freshly formed SOA. Overall, Fig. 2 clearly shows that large differences in chemical composition exist between the two seasons in the Amazon rainforest. However, we did not observe significant variations at different altitudes.



370 **Figure 2: Carbon oxidation state (OSC) plots for all detected CHO species during the wet season 2018 (left) and dry season 2018 (right) at different sampling heights. Only background ions are included. The size of the data points represents the signal intensity of the corresponding peak. The color code illustrates the degree of oxygenation. The black dashed areas are related to low-volatility (LV-OOA) and semivolatile (SV-OOA) oxygenated organic aerosol and biomass-burning organic aerosol (BBOA). Insets: vectors corresponding to key classes of reactions of atmospheric organics: functionalization (addition of polar functional groups),**



375 fragmentation (cleavage of C–C bonds), and oligomerization (covalent association of two organic species). The combination of these reaction types leads to complex movement through (-the OSC–carbon number-) space; however, the inevitable increase in OSC with atmospheric oxidation implies that, given enough time, organics will generally move up and to the right (blue arrows). Insets based on Kroll et al., 2011.

### 3.3 Variable OA characteristics

The occurrence of variable component contributions to the chemical composition of OA is attributed to irregular atmospheric events, which are presumably caused by varying meteorological conditions, i.e. uncommon wind direction, long-range transported plumes or fires or anthropogenic pollution nearby. Compounds that were only detected once in the respective data set were excluded, as they were not considered representative. As already mentioned, the previously discussed background compounds were not taken into account for the group of variable compounds defined here. The remaining signals were assigned according to the sampling time during the day (7:00 - 17:00 local time, UTC-4h) and night (17:00 - 7:00 local time, UTC-4).  
 385 The results and trends discussed in this chapter are considered representative for both years (2018 and 2019) and for clarity, the graphs for 2019 are shown in the supplement (Figure S 11, Figure S 12).

#### 3.3.1 Molecular tracer compounds of individual events

In this section, Van Krevelen and OSC diagrams are discussed with the aim of identifying molecular tracer components that can be associated with individual meteorological or atmospheric chemical events. Representative VK diagrams for the seasons in 2018 are shown in Figure 3. The respective diagrams of the wet and dry season 2019 are shown in Figure S11. With the non-targeted approach used in this study, only small altitude-dependent differences in the chemical composition of OA could be observed. Therefore, only VK diagrams of samples at 320 m altitude are discussed in this section. For better understanding, the VK diagrams were divided into five areas: *I* for very highly oxidized organic compounds, *II* for highly oxidized compounds, *III* for intermediately oxidized compounds, *IV* for oxidized unsaturated organic compounds and *V* for highly unsaturated organic compounds. The five areas were defined according to Zhang et al., 2021.

**(I) Very highly oxidized organic compounds:** Area *I* shows very highly oxidized organic compounds, with isoprene oxidation products being a distinctive feature. Since less wet deposition of aerosol particles occurred due to less precipitation events during the dry season 2018, a greater number of compounds were identified during the dry season 2018 than during the wet season 2018. This result is consistent with the particle mass and number concentrations (Figure S 4, Figure S 5) observed during these campaigns. No significant differences were observed for the corresponding daytime and nighttime samples for the wet season 2018. C<sub>5</sub>H<sub>12</sub>O<sub>4</sub> (*m/z* 136.0662) was detected in all samples from all seasons and identified as 2-methyltetrole, a prominent product of isoprene oxidation (Claeys et al., 2004). A large number of CHOS compounds were detected during the dry season 2018. More than 85 % of the CHOS molecules detected showed an O/S ratio  $\geq 4$ , indicating the presence of at least one sulfate functional group. Species with O/C  $\geq 1$  and H/C  $\geq 2$  with highly oxygenated C4 and C5 backbones were particularly prominent. Their structures emphasize that isoprene is the main precursor for S-containing OA at ATTO. C<sub>5</sub>H<sub>12</sub>O<sub>7</sub>S (*m/z* 215.0231, IEPOX-OS) and C<sub>5</sub>H<sub>10</sub>O<sub>7</sub>S (*m/z* 213.0075) were detected in filter samples from all four campaigns and showed the highest intensities. Both structures have already been identified as isoprene-derived OS and correlate with increased sulfate concentrations during dry periods. The latter can be attributed to the long-range transport of anthropogenic emissions (Andreae et al., 2015). In addition, higher CHOS signal intensities were observed in all nocturnal samples than in the corresponding daytime samples in the dry season 2018, which shows a pronounced diurnal variation and can be explained by the temperature dependence of gas-particle partitioning (Kourtchev et al., 2014b; Gómez-González et al., 2012).

**(II) Highly oxidized organic compounds:** In general, area *II* is characterized by highly oxidized organic species like late monoterpene oxidation products due to oxidative aging or higher generation oxidation products (Zhang et al., 2021). The dry season 2018 shows a higher number of compounds than the wet season 2018, indicating more aged organic aerosol. This is also underlined by an increased number of LV-OOA species in the OSC plots in Figure 4. An intense ion signal with *m/z* 203.0562 (C<sub>8</sub>H<sub>12</sub>O<sub>6</sub>) could be assigned to 3-methyl-1,2,3-butanetricarboxylic acid (MBTCA) by comparison with an



authentic standard. MBTCA is a well-established tracer compound for aged biogenic SOA formed by the photooxidation of  $\alpha$ - and  $\beta$ -pinene (Szmigielski et al., 2007; Zhang et al., 2010). Similarly, two detected CHONS compounds at  $m/z$  294.0654 ( $C_{10}H_{17}O_7NS$ ) and  $m/z$  296.0446 ( $C_9H_{15}O_8NS$ ) were associated with aged SOA, which were previously identified as oxidation products of  $\alpha$ -pinene,  $\beta$ -pinene and limonene (Surratt et al., 2008). The O/(N+S) ratio  $\geq 3.5$  allows for the presence of both -OSO<sub>3</sub>H and -ONO<sub>2</sub> functional groups and assignment as nitrooxy organosulfates (NOS). Similar to the higher concentrations of very highly oxidized CHOS species (**I**), highly oxidized (**II**) CHONS species also show increased concentrations in dry periods and high correlations with SO<sub>2</sub> levels, but also NO<sub>x</sub> concentrations (increased NO<sub>x</sub> and black carbon equivalent concentrations (BC<sub>e</sub>) in the dry season 2018; Figure S6 and S13). This underlines the importance of anthropogenic emissions reaching the ATTO site by long-distance transport and changing the chemical composition of organic aerosols by mixing biogenic and anthropogenic sources.

The molecular assignment of two further ions,  $m/z$  161.0455 ( $C_6H_{10}O_5$ ) and  $m/z$  129.0194 ( $C_5H_6O_4$ ) with increased concentrations in the dry season clearly shows a connection with biomass burning activities. The overall burning activity in the basin was significantly lower in the wet season 2018 compared to the dry season 2018 (Table S 3).  $C_6H_{10}O_5$  can be assigned to 1,6-anhydro- $\beta$ -D-glucopyranose (Levogluconan) by comparison with authentic standard substances. Levogluconan is a generally recognized product of cellulose pyrolysis that is used as a marker compound for biomass burning activities (Simoneit et al., 1999; Nolte et al., 2001). However,  $C_5H_6O_4$  can be explained less clearly. A compound with this molecular formula was found as an oxidation product of the reaction of 3-methylfuran with NO<sub>3</sub> radicals (Joo et al., 2019), while furans themselves were detected as products of cellulose combustion (Mettler et al., 2012). The  $C_5H_6O_4$  molecule observed here showed higher concentrations in dry season samples (higher number of fires) and in night samples (nitrate radical chemistry), supporting the hypothesis that the reaction of 3-methylfuran with NO<sub>3</sub> radicals is a source of this compound. However, the C<sub>5</sub> backbone can also suggest isoprene as potential precursor, which can also form  $C_5H_6O_4$  according to photooxidation experiments in chamber studies (Nguyen et al., 2011; Clark et al., 2013).

**(III) Intermediately oxidized organic compounds:** Area **III** mostly consists of first-generation oxidation products of monoterpenes and sesquiterpenes that are intermediately oxidized (Zhang et al., 2021). Again, the dry season 2018 is characterized by a higher number and concentration of compounds than the wet season 2018 while no significant differences are observed between the daytime and nighttime samples. The compounds are characterized by aliphatic species that can be attributed to mixed anthropogenic and biogenic sources (Henze et al., 2008; Kourtev et al., 2013). A prominent ion was observed at  $m/z$  185.0819, which was assigned to the molecular formula  $C_9H_{14}O_4$ . The compounds with this molecular formula showed multiple signals in the LC-MS analysis, indicating the presence of several isomeric structures. One signal was identified as pinic acid (PA) from an authentic standard compound. The additional signals are likely to be oxidation products of other monoterpenes, such as  $\beta$ -pinene, limonene and  $\Delta^3$ -carene (Jenkin, 2004; Chen and Griffin, 2005; Hammes et al., 2019). In contrast to MBTCA, pinic acid is an oxidation product that is already formed during the first oxidation steps of  $\alpha$ -pinene and can therefore be used as a tracer for freshly formed SOA. Later generation products, such as MBTCA, were more concentrated in the dry seasons, indicating more processed SOA particles, while PA was predominant in the wet periods. The OSC analysis in Figure 4 shows that the dry season 2018 has pronounced signals at small numbers of C atoms with high O/C ratios, whereas the wet season 2018 is characterized by pronounced SV-OAA species, supporting the different seasonal variation of different generations.

**(IV) Oxidized unsaturated organic compounds:** This area is mainly characterized by unsaturated hydrocarbons with a low oxygen content. Most of these compounds are classified as CHON, CHOS and CHONS with  $X_c \geq 2.5$ , indicating aromatic molecular structures. The dry season 2018 shows a higher diversity of compounds whereas the wet season 2018 consists of a lower number of compounds mainly dominated by CHO species. At nighttime during the wet season 2018, the concentrations of CHO compounds are reduced. In contrast, the nighttime samples from the dry season 2018 do not exhibit a similar trend in concentrations. However, the wet season of 2018 shows a higher presence of CHON species during nighttime compared to



460 daytime samples. The most intense ion signals in the dry season 2018  $m/z$  154.0146 ( $C_6H_5NO_4$ , 4-nitrocatechol),  $m/z$  168.0301 ( $C_7H_7NO_4$ , methyl-nitrocatechols) and  $m/z$  185.0457 ( $C_8H_9NO_4$ , dimethyl-nitrocatechols) can be associated with nitroaromatic compounds, which are also considered markers for biomass burning OA (Iinuma et al, 2010; Claeys et al, 2012; Kitanovski et al, 2012; Kahnt et al, 2013; Siemens et al., 2023). Kourtchev and coworkers (Kourtchev et al., 2016) also observed elevated concentrations of these compounds in the Amazon region during the period when numerous forest fires occurred. In contrast, 465 no nitrocatechols were detected for the wet season 2018. However,  $C_6H_5NO_4$  was the only compound identified as a background species during the dry season 2018 (Figure 1), suggesting a lower SOA contribution from  $C_7H_7NO_4$  and  $C_8H_9NO_4$  at ATTO.

**(V) Highly unsaturated organic compounds:** Area *V* is predominantly composed of highly unsaturated organic compounds that are combustion-related (Zhang et al., 2021). The number of compounds and the variety of species is enhanced for the dry 470 season 2018 compared to the wet season 2018. This trend is also reflected in the BBOA areas in Figure 4. Furthermore, black carbon equivalent concentrations (BCe) were enhanced during the dry season 2018 compared to the wet season 2018 (Figure S13). While the wet season 2018 shows mainly CHO species with decreased concentrations during nighttime, the dry season 2018 is dominated by CHOS and CHONS species and an increased number of CHON compounds during nighttime.

475 The wet season of 2019 stands out and emphasizes the influence of aerosol composition on ATTO through individual events. The number of components and their intensity are both increased in areas *I-V* for the wet season 2019 in comparison to the wet season 2018, as well as in comparison to the dry season 2019 (Figure S11). The wet season 2019 generally exhibits increased concentrations of CHON and CHO species in comparison to the dry season of the same year. The concentrations of OS related to isoprene are of a similar magnitude to those observed during the dry seasons of 2019 and 2018. In particular, 480 area *V* in Figure S11 and the BBOA area in Figure S12 demonstrate that the wet season 2019 was significantly influenced by biomass burning and combustion activities. This is also reflected by enhanced BC concentrations (Figure S13). While the background OA characterization still exhibits clear wet season characteristics (low concentration in the BBOA area, dominance of early monoterpene oxidation products, lower significance of aerosol aging effects in Figure S10 and missing signals in area *V* in Figure S7), it becomes evident that, with the inclusion of individual events, significantly polluted conditions in the wet 485 season 2019 could be discerned, which markedly alter the aerosol composition. This atypical behavior suggests a substantial influence from intensified forest fires or combustion activities occurring either upwind of the ATTO site or in its vicinity in the wet season 2019 (Table S3). Additionally, emissions from biomass burning in the Sahel savanna regions, transported across the Atlantic Ocean (Figure S3), could have contributed to the observed aerosol characteristics (Holanda et al., 2020; Holanda et al., 2023).



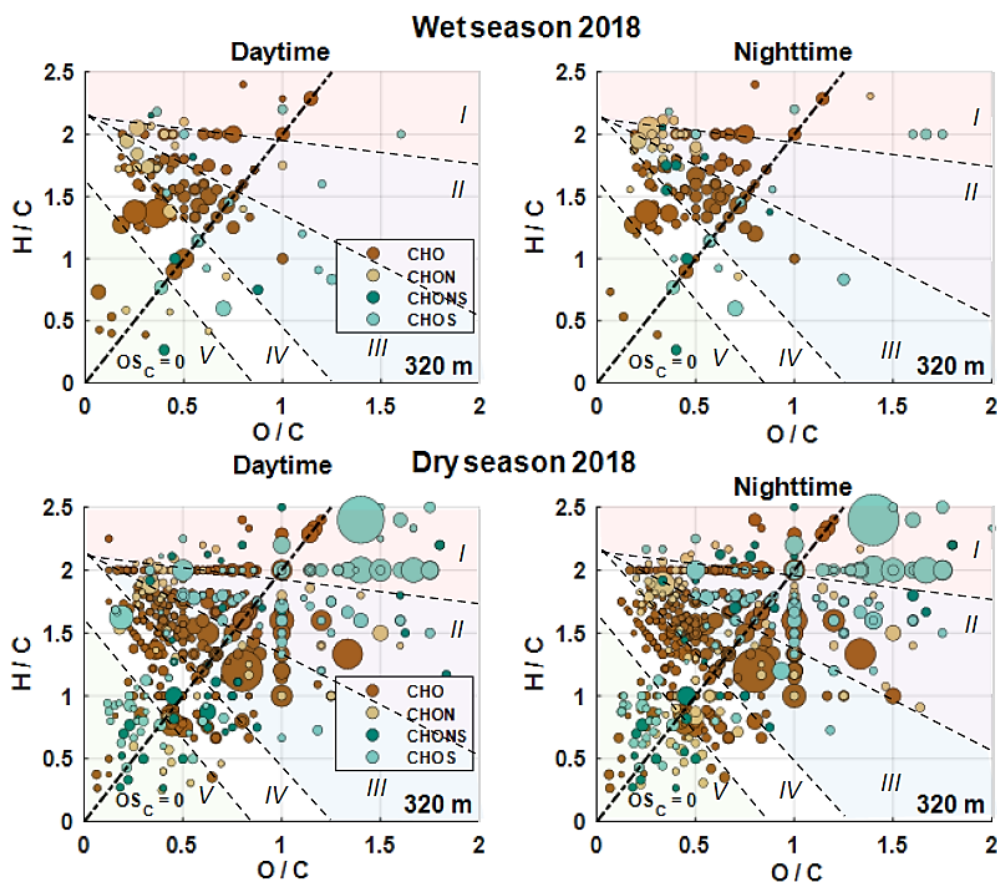


Figure 3: Van Krevelen plots from the wet season 2018 (upper panel) and dry season 2018 (lower panel) during daytime (left panel) and nighttime (right panel) at 320 m height. Included are only molecular formulae that were present in more than one of the samples, respectively. The background signals are subtracted. The size of the data points represents the signal intensity of the corresponding peak. The four subgroups CHO, CHON, CHONS and CHOS are distinguished with different colors. Compounds located on the black dashed line have an average carbon oxidation state of 0 ( $OSC = 0$ ). The VK diagram was divided into five areas: I for very highly oxidized organic compounds, II for highly oxidized compounds, III for intermediately oxidized compounds, IV for oxidized unsaturated organic compounds and V for highly unsaturated organic compounds. The five areas were defined according to Zhang et al., 2021. Area (I) is mainly characterized by CHOS molecules with at least one sulfate functional group and C4 and C5 backbones. Area (II) is dominated by highly oxidized compounds representing aged OA and biomass burning products. Area (III) shows mainly aliphatic species. Area (IV) is dominated by unsaturated hydrocarbons with low oxygen content and aromatic structures while area (V) shows mainly combustion related species.

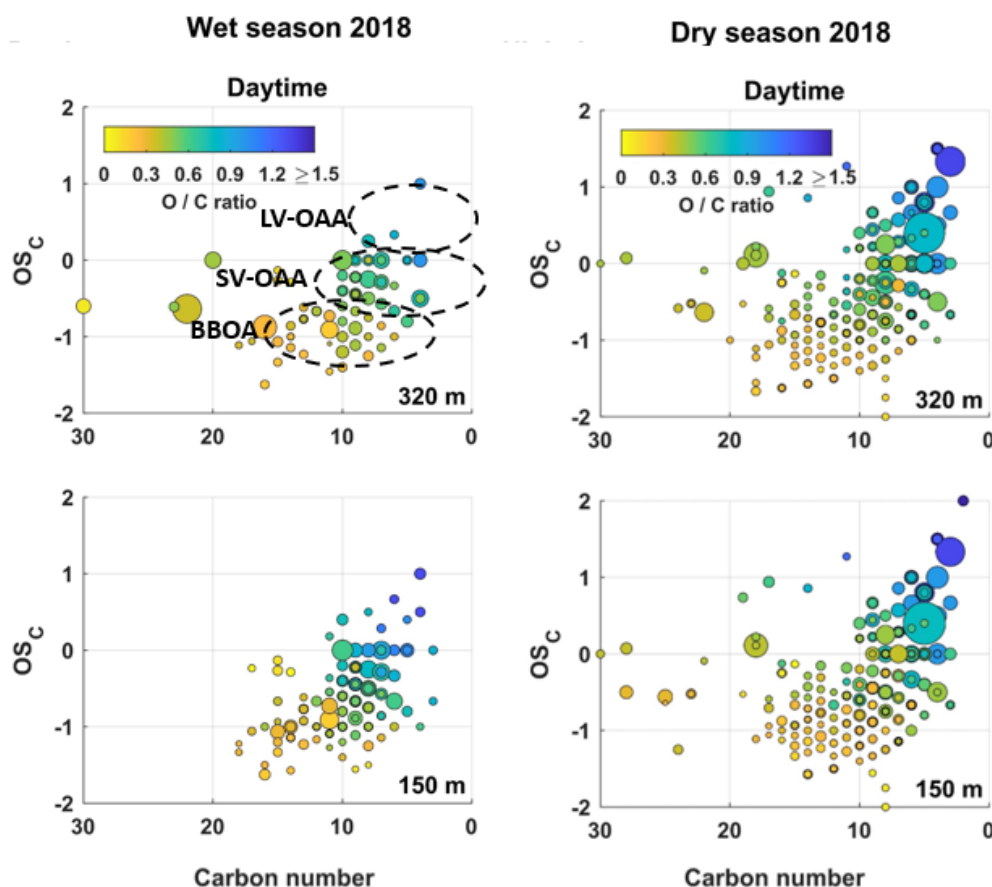


Figure 4: Carbon oxidation state (OSC) plots for all detected CHO species during the wet season 2018 at daytime (left) and dry season 2018 (right) at daytime at 150 m and 320 m sampling height. Included are only molecular formulae that were present in more than one of the samples, respectively. The background signals are subtracted. The size of the data points represents the signal intensity of the corresponding peak. The color code illustrates the degree of oxygenation. The black dashed areas are related to low-volatility (LV-OAA), semivolatile (SV-OAA) oxygenated organic aerosol and biomass burning organic aerosol (BBOA).

### 3.3.2 Saturation vapor pressure

The saturation vapor pressure  $C^0$  is an important thermodynamic property that regulates the gas-to-particle partitioning properties of organic molecules and enables their classification as VOCs, intermediate volatile organic compounds (IVOCs), semi-volatile OCs (SVOCs), low-volatility OCs (LVOCs) and extremely low-volatility OCs (ELVOCs) (Pankow, 1994; Odum et al., 1996; Murphy et al., 2014). The relationship between molecular weight, chemical composition and saturation vapor pressure has already been used to describe the chemical evolution of organic aerosols (Shiraiwa et al., 2014; Li et al., 2016). Figure 5 compares 2-D maps of molecular weight plotted against saturation vapor pressure of the organic species measured in this study from the dry and wet season 2018. Nearly all CHONS compounds are located in the LVOC/ELVOC range, and it is clear that many of the additional compounds occurring in the dry season have very low volatility, indicated by high molecular weights on the one hand, and a more oxidized (aged) character compared to the wet season composition on the other. Increased nitrogen oxide and  $\text{SO}_2$  concentrations and thus the formation of N- and S-functionalized oxidation products, but also a lower removal by precipitation and thus longer residence times in the atmosphere could explain these differences between wet and dry season. The seasonal difference suggest they are part of the hemispheric wide burning signature in the dry season. Several



high molecular weight compounds with C8-C10 or C17-C20 backbones have also been identified as LVOC/ELVOC, suggesting oligomeric structures based on isoprene and monoterpene precursors. It is hypothesized that these products are low volatile due to the incorporation of additional functional groups and the increase in carbon number in the molecular structure (Kroll and Seinfeld, 2008; Daumit et al., 2013). Two prominent ion signals at  $m/z$  333.0859 ( $C_{10}H_{22}O_{10}S$ ) and  $m/z$  357.1557 ( $C_{17}H_{26}O_8$ ) have already been observed in chamber studies with isoprene and  $\alpha$ -pinene (Surratt et al., 2008; Kristensen et al., 2013). In addition to oligomeric structures derived from isoprene and monoterpene precursors, components with the highest molecular weight (MW) of  $500 < MW < 600$  g/mol were also found in the dry season 2018. These signals could indicate oxygenated dimers of sesquiterpene oxidation products previously identified in chamber simulation experiments from  $\beta$ -caryophyllene ozonolysis (Gao et al., 2022). The authors investigated the formation of SOA in the presence and absence of nitrogen oxides at different temperatures. At a temperature of 313 K and the absence of nitrogen oxides, monomers (mainly  $C_{14-15}H_{22-24}O_{3-7}$ ) and dimers (mainly  $C_{28-30}H_{44-48}O_{5-9}$ ) could be detected. In the presence of nitrogen oxides, which is more in line with the dry season 2018 conditions, most organonitrates were found as monomers with a C15 skeleton with a nitrate group. Nevertheless, purely organic species without nitrogen atoms (C20, C35) were newly formed in the presence of nitrogen oxides, supporting the results presented here. Most oligomers were detected in filter samples from dry season campaigns, suggesting a stronger contribution of the oligomerization reaction to SOA during these periods. These trends indicate that SOA formation and reactions make a greater contribution to ELVOC species during the dry seasons than during the wet seasons.

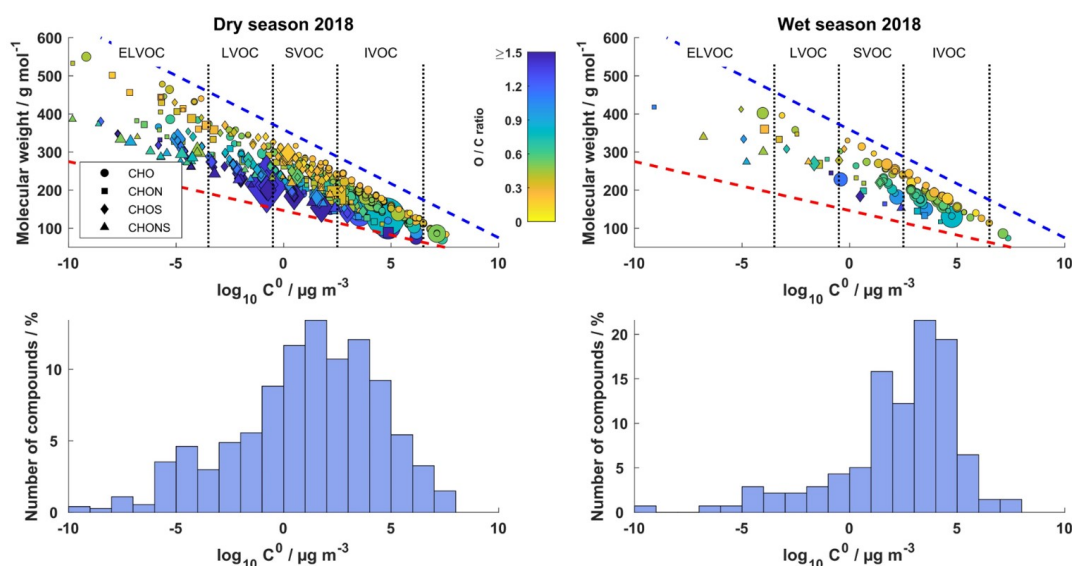
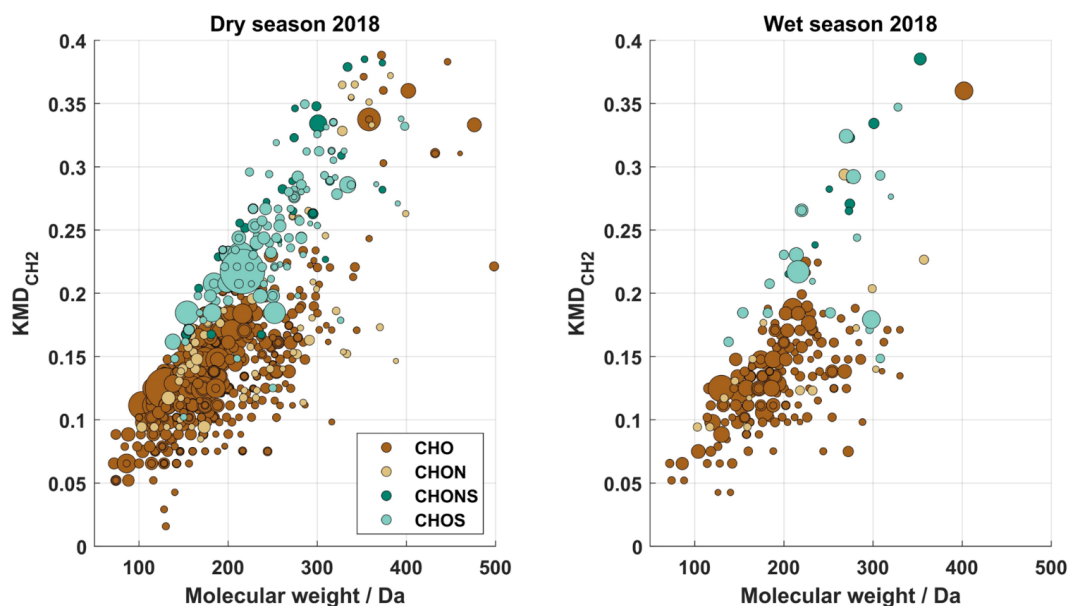


**Figure 5:** Molecular classification of organic species for the dry season 2018 (left) and the wet season 2018 (right) according to their saturation vapor pressure  $C^0$ . The color code describes the degree of oxygenation. The blue dashed line indicates linear alkanes  $C_nH_{2n+2}$ , while the red dashed line represents sugar alcohols  $C_nH_{2n+2}O_n$  according to Li et al. (2016). The lower panel shows the distribution of all detected compounds among the respective classes.

### 3.3.3 Kendrick mass analysis

Kendrick mass analysis is a valuable visualization tool for complex organic mixtures and was introduced by Kendrick (1963) and later refined by Hughey et al. (2001). This technique has already been used to characterize organic aerosol samples (Lin et al., 2012; Rincón et al., 2012; Kourtchev et al., 2013). It enables the assignment of all signals of a homologous series when the elemental composition of a compound has been identified (Nizkorodov et al., 2011). Figure 6 compares the  $KMD_{CH_2}$  diagrams (see eq. 2.5 and 2.6) for the dry and wet seasons in 2018. Compounds differing only in their number of  $CH_2$  units have the same  $KMD$  values. Homologous series can be identified as horizontal lines in  $KMD$  plots.



550 **Figure 6:** CH<sub>2</sub>-Kendrick diagrams for all signals detected at 150 m during the dry season 2018 (left) and the wet season 2018 (right), respectively. The size of the data points represents the signal intensity of the corresponding peak. The four subgroups are distinguished with different colors.

As mentioned above, the dry season was characterized by biomass burning and the occurrence of aged organic aerosol components, resulting in large-membered homologous series of CHO compounds with higher MW than in the wet season.

555 Compounds with  $KMD_{CH_2} \leq 0.11$  appear to be unsaturated carboxylic acids with the general molecular formulae  $C_nH_{2n}O_2$ ,  $C_nH_{2n}O_3$ ,  $C_nH_{2n-2}O_2$  and  $C_nH_{2n-2}O_4$ . The elemental composition suggests fatty acids, which have been described in OA-related studies as essential compounds of marine and terrestrial vegetation (Stephanou and Stratigakis, 1993; Rincón et al., 2012; Kourtechev et al., 2014b). Thus, long-range transport of marine aerosols or BBOA could explain the greater abundance of fatty acids during the dry season (Oros and Simoneit, 2001; Tervahattu et al., 2002). In addition, a large number of CHOS

560 compounds with  $KMD_{CH_2} \geq 0.21$  were detected exclusively during the dry season. Similar results were reported by Kourtechev et al. (2016), who found a larger number of homologous series of CHOS compounds in aerosol samples affected by anthropogenic emissions. These species are presumably highly oxygenated organosulfates, which are probably formed by heterogeneous reactions on acidic sulfate particles.

Another interesting ion was detected at  $m/z$  186.1135 ( $C_9H_{17}NO_3$ ) with high signal intensities, especially during the dry season

565 2018. This compound has already been observed in biomass burning chamber experiments and field measurements in the Amazon rainforest (Laskin et al., 2009; Kourtechev et al., 2016). In the present study, Kendrick mass analysis revealed evidence of a homologous series, which is shown in the KMD plot in Figure 7. The general molecular formula can be described as  $C_nH_{2n-1}NO_3$ , where  $n$  ranges from 3 to 17 depending on the filter sample. The elemental composition initially suggested a nitrooxy functional group ( $-ONO_2$ ), but  $MS^2$  experiments (Figure S 14) did not show the typical nitrate fragment. Instead, the

570 observed fragments indicated the presence of a carbamate functional group ( $R-NH-COOH$ ). Due to their zwitterionic structure, these species could be relevant for condensed phase chemistry in the atmosphere, similar to amino acids (Mopper and Zika, 1987; Milne and Zika, 1993; McGregor and Anastasio, 2001; Barbaro et al., 2011).

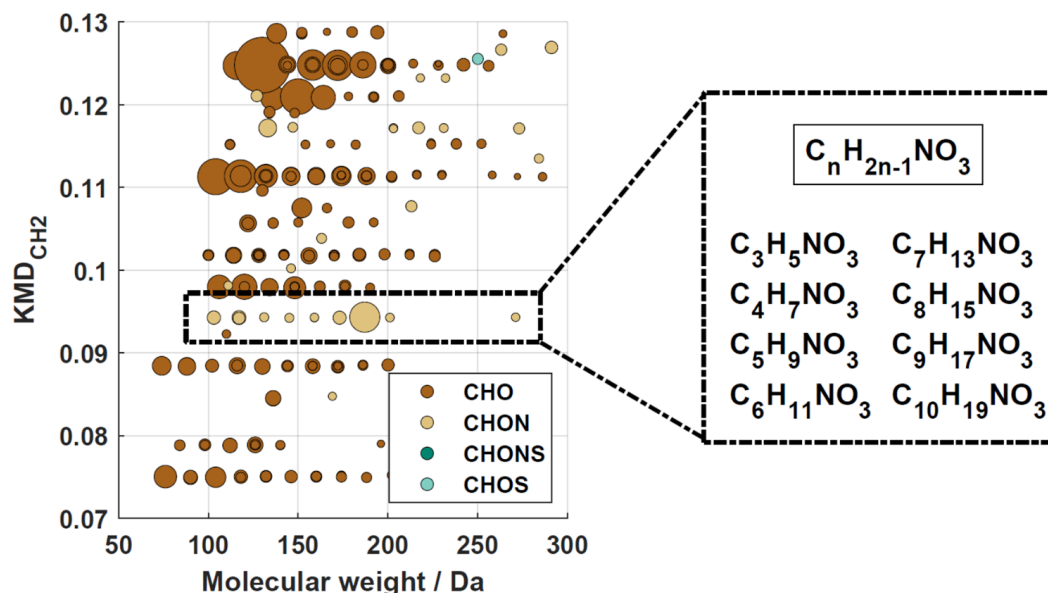


Figure 7: Kendrick mass defect diagram for the dry season 2018. The size of the data points represents the signal intensity of the corresponding peak. The four subgroups are distinguished with different colors. The dashed box highlights a homologous series of CHON compounds with a molecular formula of  $C_nH_{2n-1}NO_3$  with  $n = (3 - 17)$ , potentially related to biomass burning emissions.

#### 4 Conclusion

The organic chemical composition of atmospheric OA particles from the Amazon rainforest was investigated at the ATTO station using high-resolution MS in combination with an UHPLC system. Between 2018 and 2019, a total of four measurement campaigns were carried out, including two dry and wet seasons, with "clean" wet periods and "polluted" dry periods. This allows conclusions to be drawn about seasonal influences in a unique ecosystem that is characterized by the complex interaction of numerous emission sources. In this analysis, a distinction was made between background compounds with a relatively low variability over time, and compounds with a much higher variability in their concentrations.

The results show a high fraction of isomeric structures in each data set, highlighting the need to use chromatographic separation methods for molecular identification of the aerosol components. Such an approach allows the reliable identification and quantification of a number of important marker compounds if reference compounds are available. However, the semi-quantitative determination of other compound classes is also possible, particularly by reducing ion suppression. The majority of compounds measured in both seasons had molecular weights (MW) below 250 Da. In addition, the analysis of the dry season samples showed signals in the oligomeric range between 300 and 450 Da with lower intensities. In general, the background molecular composition of organic aerosols at ATTO showed a clear seasonality with large differences between the dry and wet seasons. A considerable number of suitable marker compounds for different SOA sources were identified. The most important sources of background SOA at ATTO were the oxidation of isoprene and monoterpenes at both, high and low NO<sub>x</sub> concentrations and the formation of organosulfates. The results show that isoprene is the main precursor for S-containing SOA components at ATTO. The formation of isoprene OS probably occurs through the reactive uptake of IEPOX on acidic sulfate particles. It is assumed that in the wet season the sulfate particles reach the ATTO station mainly by long-range transport of marine aerosol, while in the dry season direct anthropogenic sources are also likely to be present. Furthermore, earlier studies showed that organic sulfur emissions from soils increase with higher soil water content what indicates a stronger organosulfur soil source from the forest itself in the wet seasons. Isoprene organosulfates can have both, purely biogenic and anthropogenic



sources, whereby the biogenic sources appear to have a greater influence if the background OA composition is taken into account. This is further supported by the observation that the CHOS subgroup accounted for  $(8 \pm 7)$  % in the wet season compared to only  $(3 \pm 2)$  % in the dry season. Other dominant SOA groups that characterized the background were aromatic compounds whose source was most likely biomass burning. Thus, various oxygenated and nitrated hydrocarbons and oxidized polycyclic compounds showed significantly higher concentrations during the dry seasons. The evaluation of carbon oxidation states shows that LV-OOA and BBOA were the predominant and highly concentrated species in the dry seasons, while SV-OOA dominated in the wet seasons. We assume that a significant proportion of LV-OOA is formed by the aging and chemical processing of SOA components.

High signal intensities of nitroxyorganosulfates were observed in the dry seasons 2018 and 2019 as well as in the wet season 2019, whereby these were particularly derived from monoterpene precursors and correlated with the increased occurrence of fires and the  $\text{SO}_2$  and  $\text{NO}_x$  concentrations. Noteworthy are the low vapor pressures of the CHONS compounds, which therefore make a significant contribution to ELVOCs. In addition, we find evidence of oligomeric structures of biogenic SOA components, as well as dimers of sesquiterpene oxidation products, which could also contribute to the ELVOC fraction. At the same time, a large fraction of BBOA contributes to the total OA, as shown by the high  $X_c$  values. Consequently, unsaturated and aromatic compounds such as nitrocatechols and nitrophenols were mainly attributed to deforestation fires, which occurred mainly during the dry periods. Interestingly, the chemical composition of OA particles from the 2019 wet season revealed a similar OA composition as in the dry season, suggesting that combustion emissions played a larger role in the wet season 2019. Fossil fuel combustion in Europe or strong biomass burning in the Sahel savanna regions could be responsible via long-distance transportation across the Atlantic. Follow up studies to address these different long-range transport scenarios in dedicated case studies, providing a more detailed understanding of their respective contributions are in preparation.

#### Data availability

The data sets are available at upon registration at <https://www.attodata.org> (last access: 25 January 2022), and more information can be given by Thorsten Hoffmann ([t.hoffmann@uni-mainz.de](mailto:t.hoffmann@uni-mainz.de)).

#### Author contributions

DL and SH contributed equally. DL, SH and TH planned and designed the study. DL conducted the aerosol sampling, the sample preparation and analysis, the evaluation and wrote the manuscript. SH conducted the method validation of sample preparation and analysis, the evaluation and wrote the manuscript. NZ helped to collect the aerosol samples and revised the manuscript. LK, BH, JW, CP, and SW provided the SMPS and trace gas data. The meteorological data was provided by MS. MCS and UP provided scientific input and revised the manuscript. All authors contributed to the discussion of the results as well as the finalization of the manuscript.

#### Competing interests

The contact author has declared that none of the authors has any competing interests.

#### Financial support

This research has been supported by the German Federal Ministry of Education and Research (BMBF, grant no. 01LK1602D); the Brazilian Ministério da Ciência, Tecnologia e Inovação (MCTI/FINEP); the Amazon State University (UEA); Fundação de Amparo à Pesquisa do Estado do Amazonas (FAPEAM); LBA/INPA; and SDS/CEUC/RDS-Uatumã and the German Research Foundation (Deutsche Forschungsgemeinschaft DFG: HO 1748/19–1; HO 1748/23–1; TRR 301 – Project-ID 428312742).





This open-access publication was funded by Johannes Gutenberg University Mainz.

645

### Acknowledgments

For the operation of the ATTO site, we acknowledge the support by the German Federal Ministry of Education and Research (BMBF Contract 01LK1602D) and the Brazilian Ministério da Ciência, Tecnologia e Inovação (MCTI/FINEP) as well as the  
650 Amazon State University (UEA), FAPEAM, LBA/INPA, and SDS/CEUC/RDS-Uatumã. We also acknowledge the support of the Max Planck Society, and the Max Planck Graduate Center with the Johannes Gutenberg University Mainz (MPGC) and the Instituto Nacional de Pesquisas da Amazonia (INPA). Furthermore, we thank Florian Ditas and Maria Prass for help providing SMPS data. Particularly, we would like to thank the ATTO team members including Susan Trumbore, Alberto Quesada, Bruno Takeshi, Reiner Ditz, Stefan Wolff, Björn Nillius, Fernando Morais, Thomas Klimach, Roberta Pereira de  
655 Souza, Jürgen Kesselmeier, Andrew Crozier, Sam Jones, Delano Campos, Juarez Viegas, Sipko Bulthuis, Francisco Alcinei Gomes da Silva, Isabella Diogenes, Hermes Braga Xavier, Nagib Alberto de Castro Souza, Antonio Huxley Melo Nascimento, Valmir Ferreira de Lima, Feliciano de Souza Coelho, André Luiz Matos, Wallace Rabelo Costa, Amauri Rodrigues Perreira, Adir Vasconcelos Brandão, Davirley Gomes Silva, Thomas Disper, Torsten Helmer, Steffen Schmidt, Uwe Schulz, Uwe Schultz, Karl Kübler, Olaf Kolle, Martin Hertel, Kerstin Hippler, Steffen Schmidt and all further colleagues involved in the  
660 technical, logistical, and scientific support.





## References

- 665 Andreae, M. O., Acevedo, O. C., Araújo, A., Artaxo, P., Barbosa, C. G. G., Barbosa, H. M. J., Brito, J., Carbone, S., Chi, X.,  
 Cintra, B. B. L., da Silva, N. F., Dias, N. L., Dias-Júnior, C. Q., Ditas, F., Ditz, R., Godoi, A. F. L., Godoi, R. H. M.,  
 Heimann, M., Hoffmann, T., Kesselmeier, J., Könemann, T., Krüger, M. L., Lavric, J. V., Manzi, A. O., Lopes, A.  
 P., Martins, D. L., Mikhailov, E. F., Moran-Zuloaga, D., Nelson, B. W., Nölscher, A. C., Santos Nogueira, D.,  
 Piedade, M. T. F., Pöhlker, C., Pöschl, U., Quesada, C. A., Rizzo, L. V., Ro, C.-U., Ruckteschler, N., Sá, L. D. A.,  
 670 Oliveira Sá, M. de, Sales, C. B., dos Santos, R. M. N., Saturno, J., Schöngart, J., Sörgel, M., Souza, C. M. de, Souza,  
 R. A. F. de, Su, H., Targhetta, N., Tóta, J., Trebs, I., Trumbore, S., van Eijck, A., Walter, D., Wang, Z., Weber, B.,  
 Williams, J., Winderlich, J., Wittmann, F., Wolff, S., and Yáñez-Serrano, A. M.: The Amazon Tall Tower  
 Observatory (ATTO): Overview of pilot measurements on ecosystem ecology, meteorology, trace gases, and aerosols,  
*Atmos. Chem. Phys.*, 15, 10723–10776, <https://doi.org/10.5194/acp-15-10723-2015>, 2015.
- 675 Artaxo, P. et al.: Tropical and Boreal Forest – Atmosphere Interactions: A Review. *Tellus B: Chemical and Physical  
 Meteorology*, 74, 24–163, <https://doi.org/10.16993/tellusb.34>, 2022.
- Artaxo, P., Rizzo, L. V., Brito, J. F., Barbosa, H. M. J., Arana, A., Sena, E. T., Cirino, G. G., Bastos, W., Martin, S. T., and  
 Andreae, M. O.: Atmospheric aerosols in Amazonia and land use change: From natural biogenic to biomass burning  
 conditions, *Faraday Discuss.*, 165, 203, <https://doi.org/10.1039/c3fd00052d>, 2013.
- 680 Artaxo, P.: Physical and chemical properties of aerosols in the wet and dry seasons in Rondônia, Amazonia, *J. Geophys. Res.*,  
 107, 1052, <https://doi.org/10.1029/2001JD000666>, 2002.
- Baccini, A., Goetz, S. J., Walker, W. S., Laporte, N. T., Sun, M., Sulla-Menashe, D., Hackler, J., Beck, P. S. A., Dubayah, R.,  
 Friedl, M. A., Samanta, S., and Houghton, R. A.: Estimated carbon dioxide emissions from tropical deforestation  
 improved by carbon-density maps, *Nature Clim. Change*, 2, 182–185, <https://doi.org/10.1038/nclimate1354>, 2012.
- 685 Badertscher, M., Bischofberger, K., Munk, M. E., and Pretsch, E.: A novel formalism to characterize the degree of unsaturation  
 of organic molecules, *J. Chem. Inf. Comput. Sci.*, 41, 889–893, <https://doi.org/10.1021/ci000135o>, 2001.
- Bateman, A. P., Walser, M. L., Desyaterik, Y., Laskin, J., Laskin, A., and Nizkorodov, S. A.: The effect of solvent on the  
 analysis of secondary organic aerosol using electrospray ionization mass spectrometry, *Environ. Sci. Technol.*, 42,  
 7341–7346, <https://doi.org/10.1021/es801226w>, 2008.
- 690 Bates, K. H. and Jacob, D. J.: A new model mechanism for atmospheric oxidation of isoprene: global effects on oxidants,  
 nitrogen oxides, organic products, and secondary organic aerosol, *Atmos. Chem. Phys.*, 19, 9613–9640,  
<https://doi.org/10.5194/acp-19-9613-2019>, 2019.
- Baumann, K., Wietzoreck, M., Shahpoury, P., Filippi, A., Hildmann, S., Lelieveld, S., Berkemeier, T., Tong, H., Pöschl, U.  
 and Lammel, G.: Is the oxidative potential of components of fine particulate matter surface-mediated?, *Environ. Sci.*  
 695 *Pollut. Res.*, 30(6), 16749–16755. <https://doi.org/10.1007/s11356-022-24897-3>, 2023.
- Bianchi, F., Tröstl, J., Junninen, H., Frege, C., Henne, S., Hoyle, C. R., Molteni, U., Herrmann, E., Adamov, A., Bukowiecki,  
 N., Chen, X., Duplissy, J., Gysel, M., Hutterli, M., Kangasluoma, J., Kontkanen, J., Kürten, A., Manninen, H. E.,  
 Münch, S., Peräkylä, O., Petäjä, T., Rondo, L., Williamson, C., Weingartner, E., Curtius, J., Worsnop, D. R., Kulmala,  
 M., Dommen, J., and Baltensperger, U.: New particle formation in the free troposphere: A question of chemistry and  
 700 timing, *Science (New York, N.Y.)*, 352, 1109–1112, <https://doi.org/10.1126/science.aad5456>, 2016.
- Bruns, E. A., Krapf, M., Orasche, J., Huang, Y., Zimmermann, R., Drinovec, L., Močnik, G., El-Haddad, I., Slowik, J. G.,  
 Dommen, J., Baltensperger, U., and Prévôt, A. S. H.: Characterization of primary and secondary wood combustion  
 products generated under different burner loads, *Atmos. Chem. Phys.*, 15, 2825–2841, <https://doi.org/10.5194/acp-15-2825-2015>, 2015.



- 705 Burgay, F., Salionov, D., Huber, C.J., Singer, T., Eichler, A., Ungeheuer, F., Vogel, A., Schwikowski, M., Bjelic, S., Hybrid Targeted/Untargeted Screening Method for the Determination of Wildfire and Water-Soluble Organic Tracers in Ice Cores and Snow, *Anal. Chem.*, 95(30), 11456–11466, <https://doi.org/10.1021/acs.analchem.3c01852>, 2023.
- Chan, A. W. H., Kautzman, K. E., Chhabra, P. S., Surratt, J. D., Chan, M. N., Crounse, J. D., Kürten, A., Wennberg, P. O., Flagan, R. C., and Seinfeld, J. H.: Secondary organic aerosol formation from photooxidation of naphthalene and alkyl naphthalenes: implications for oxidation of intermediate volatility organic compounds (IVOCs), *Atmos. Chem. Phys.*, 9, 3049–3060, <https://doi.org/10.5194/acp-9-3049-2009>, 2009.
- 710 Chen, J. and Griffin, R.: Modeling secondary organic aerosol formation from oxidation of  $\alpha$ -pinene,  $\beta$ -pinene, and  $\gamma$ -limonene, *Atmos. Environ.*, 39, 7731–7744, <https://doi.org/10.1016/j.atmosenv.2005.05.049>, 2005.
- Chen, Y., Takeuchi, M., Nah, T., Xu, L., Canagaratna, M. R., Stark, H., Baumann, K., Canonaco, F., Prévôt, A. S. H., Huey, L. G., Weber, R. J., and Ng, N. L.: Chemical characterization of secondary organic aerosol at a rural site in the southeastern US: insights from simultaneous high-resolution time-of-flight aerosol mass spectrometer (HR-ToF-AMS) and FIGAERO chemical ionization mass spectrometer (CIMS) measurements, *Atmos. Chem. Phys.*, 20, 8421–8440, <https://doi.org/10.5194/acp-20-8421-2020>, 2020.
- 715 Chhabra, P. S., Lambe, A. T., Canagaratna, M. R., Stark, H., Jayne, J. T., Onasch, T. B., Davidovits, P., Kimmel, J. R., and Worsnop, D. R.: Application of high-resolution time-of-flight chemical ionization mass spectrometry measurements to estimate volatility distributions of  $\alpha$ -pinene and naphthalene oxidation products, *Atmos. Meas. Tech.*, 8, 1–18, <https://doi.org/10.5194/amt-8-1-2015>, 2015.
- Claeys, M., Kourtev, I., Pashynska, V., Vas, G., Vermeylen, R., Wang, W., Cafmeyer, J., Chi, X., Artaxo, P., Andreae, M. O., and Maenhaut, W.: Polar organic marker compounds in atmospheric aerosols during the LBA-SMOCC 2002 biomass burning experiment in Rondônia, Brazil: sources and source processes, time series, diel variations and size distributions, *Atmos. Chem. Phys.*, 10, 9319–9331, <https://doi.org/10.5194/acp-10-9319-2010>, 2010.
- 725 Claeys, M., Vermeylen, R., Yasmineen, F., Gómez-González, Y., Chi, X., Maenhaut, W., Mészáros, T., and Salma, I.: Chemical characterisation of humic-like substances from urban, rural and tropical biomass burning environments using liquid chromatography with UV/vis photodiode array detection and electrospray ionisation mass spectrometry, *Environ. Chem.*, 9, 273, <https://doi.org/10.1071/EN11163>, 2012.
- 730 Claeys, M., Graham, B., Vas, G., Wang, W., Vermeylen, R., Pashynska, V., Cafmeyer, J., Guyon, P., Andreae, M. O., Artaxo, P., and Maenhaut, W.: Formation of secondary organic aerosols through photooxidation of isoprene, *Science (New York, N.Y.)*, 303, 1173–1176, <https://doi.org/10.1126/science.1092805>, 2004.
- Clark, C. H., Nakao, S., Asa-Awuku, A., Sato, K., and Cocker, D. R.: Real-Time Study of Particle-Phase Products from  $\alpha$ -Pinene Ozonolysis and Isoprene Photooxidation Using Particle into Liquid Sampling Directly Coupled to a Time-of-Flight Mass Spectrometer (PILS-ToF), *Aerosol Sci. Technol.*, 47, 1374–1382, <https://doi.org/10.1080/02786826.2013.844333>, 2013.
- Daumit, K. E., Kessler, S. H., and Kroll, J. H.: Average chemical properties and potential formation pathways of highly oxidized organic aerosol, *Faraday Discuss.*, 165, 181–202, <https://doi.org/10.1039/c3fd00045a>, 2013.
- 740 Donahue, N. M., Epstein, S. A., Pandis, S. N., and Robinson, A. L.: A two-dimensional volatility basis set: 1. organic-aerosol mixing thermodynamics, *Atmos. Chem. Phys.*, 11, 3303–3318, <https://doi.org/10.5194/acp-11-3303-2011>, 2011.
- Eddingsaas, N. C., Loza, C. L., Yee, L. D., Chan, M., Schilling, K. A., Chhabra, P. S., Seinfeld, J. H., and Wennberg, P. O.:  $\alpha$ -pinene photooxidation under controlled chemical conditions – Part 2: SOA yield and composition in low- and high-NO<sub>x</sub> environments, *Atmos. Chem. Phys.*, 12, 7413–7427, <https://doi.org/10.5194/acp-12-7413-2012>, 2012.
- 745 Florou, K., Blaziak, A., Jorga, S., Uruci, P., Vasilakopoulou, C.N., Szmigielski, R. and Pandis, S.N.: Properties and atmospheric oxidation of terebic acid aerosol, *ACS Earth Space Chem.*, 8(10), 2090–2100, <https://doi.org/10.1021/acsearthspacechem.4c00201>, 2024.



- Frauenheim, M., Offenberg, J., Zhang, Z.F., Surratt, J.D., Gold, A.: Chemical composition of secondary organic aerosol formed from the oxidation of semivolatile isoprene epoxydiol isomerization products, *Environ. Sci. Technol.*, 58(51), 22571–22582, <https://doi.org/10.1021/acs.est.4c06850>, 2024.
- Gao, L., Song, J., Mohr, C., Huang, W., Vallon, M., Jiang, F., Leisner, T., and Saathoff, H.: Kinetics, SOA yields, and chemical composition of secondary organic aerosol from  $\beta$ -caryophyllene ozonolysis with and without nitrogen oxides between 213 and 313 K, *Atmos. Chem. Phys.*, 22, 6001–6020, <https://doi.org/10.5194/acp-22-6001-2022>, 2022.
- Goldstein, A. H. and Galbally, I. E.: Known and unknown organic constituents in the Earth's atmosphere, *Environ. Sci. Technol.*, 41, 1514–1521, <https://doi.org/10.1021/es072476p>, 2007.
- Gómez-González, Y., Wang, W., Vermeulen, R., Chi, X., Neirynck, J., Janssens, I. A., Maenhaut, W., and Claeys, M.: Chemical characterisation of atmospheric aerosols during a 2007 summer field campaign at Brasschaat, Belgium: sources and source processes of biogenic secondary organic aerosol, *Atmos. Chem. Phys.*, 12, 125–138, <https://doi.org/10.5194/acp-12-125-2012>, 2012.
- Goulding, M. and Barthelm, R.: The Smithsonian atlas of the Amazon, Smithsonian Institution; Combined Academic, Washington, D.C., Chesham, 325 pp., 2003.
- Greenberg, J. P., Guenther, A. B., Pétron, G., Wiedinmyer, C., Vega, O., Gatti, L. V., Tota, J., and Fisch, G.: Biogenic VOC emissions from forested Amazonian landscapes, *Global Change Biology*, 10, 651–662, <https://doi.org/10.1111/j.1365-2486.2004.00758.x>, 2004.
- Guenther, A., Hewitt, C. N., Erickson, D., Fall, R., Geron, C., Graedel, T., Harley, P., Klinger, L., Lerdau, M., McKay, W. A., Pierce, T., Scholes, B., Steinbrecher, R., Tallamraju, R., Taylor, J., and Zimmerman, P.: A global model of natural volatile organic compound emissions, *J. Geophys. Res.*, 100, 8873, <https://doi.org/10.1029/94JD02950>, 1995.
- Hallquist, M., Wenger, J. C., Baltensperger, U., Rudich, Y., Simpson, D., Claeys, M., Dommen, J., Donahue, N. M., George, C., Goldstein, A. H., Hamilton, J. F., Herrmann, H., Hoffmann, T., Iinuma, Y., Jang, M., Jenkin, M. E., Jimenez, J. L., Kiendler-Scharr, A., Maenhaut, W., McFiggans, G., Mentel, T. F., Monod, A., Prévôt, A. S. H., Seinfeld, J. H., Surratt, J. D., Szmigielski, R., and Wildt, J.: The formation, properties and impact of secondary organic aerosol: current and emerging issues, *Atmos. Chem. Phys.*, 9, 5155–5236, <https://doi.org/10.5194/acp-9-5155-2009>, 2009.
- Hammes, J., Lutz, A., Mentel, T., Faxon, C., and Hallquist, M.: Carboxylic acids from limonene oxidation by ozone and hydroxyl radicals: insights into mechanisms derived using a FIGAERO- CIMS, *Atmos. Chem. Phys.*, 19, 13037–13052, <https://doi.org/10.5194/acp-19-13037-2019>, 2019.
- Hennigan, C. J., Sullivan, A. P., Collett, J. L., and Robinson, A. L.: Levoglucosan stability in biomass burning particles exposed to hydroxyl radicals, *Geophys. Res. Lett.*, 37, n/a-n/a, <https://doi.org/10.1029/2010GL043088>, 2010.
- Henze, D. K., Seinfeld, J. H., Ng, N. L., Kroll, J. H., Fu, T.-M., Jacob, D. J., and Heald, C. L.: Global modeling of secondary organic aerosol formation from aromatic hydrocarbons: high- vs. low-yield pathways, *Atmos. Chem. Phys.*, 8, 2405–2420, <https://doi.org/10.5194/acp-8-2405-2008>, 2008.
- Hettiyadura, A.P.S. and Laskin, A.: Quantitative analysis of polycyclic aromatic hydrocarbons using high-performance liquid chromatography-photodiode array-high-resolution mass spectrometric detection platform coupled to electrospray and atmospheric pressure photoionization sources, *J. Mass Spectrom.* 57(2), e4804, <https://doi.org/10.1002/jms.4804>, 2022.
- Hildmann, S., & Hoffmann, T.: Characterisation of atmospheric organic aerosols with one- and multidimensional liquid chromatography and mass spectrometry: State of the art and future perspectives. *TrAC Trends in Analytical Chemistry*, 175, 117698, <https://doi.org/10.1016/j.trac.2024.117698>, 2024.
- Hoffmann, D., Tilgner, A., Iinuma, Y., and Herrmann, H.: Atmospheric stability of levoglucosan: a detailed laboratory and modeling study, *Environ. Sci. Technol.*, 44, 694–699, <https://doi.org/10.1021/es902476f>, 2010.



- 790 Hoffmann, T., Huang, R.-J., and Kalberer, M.: Atmospheric analytical chemistry, *Anal. Chem.*, **83**, 4649–4664,  
<https://doi.org/10.1021/ac2010718>, 2011.
- Holanda, B. A., Pöhlker, M. L., Walter, D., Saturno, J., Sörgel, M., Ditas, J., Ditas, F., Schulz, C., Franco, M. A., Wang, Q.,  
Donth, T., Artaxo, P., Barbosa, H. M. J., Borrmann, S., Braga, R., Brito, J., Cheng, Y., Dollner, M., Kaiser, J. W.,  
Klimach, T., Knote, C., Krüger, O. O., Fütterer, D., Lavrič, J. V., Ma, N., Machado, L. A. T., Ming, J., Morais, F. G.,  
795 Paulsen, H., Sauer, D., Schlager, H., Schneider, J., Su, H., Weinzierl, B., Walser, A., Wendisch, M., Ziereis, H.,  
Zöger, M., Pöschl, U., Andreae, M. O., and Pöhlker, C.: Influx of African biomass burning aerosol during the  
Amazonian dry season through layered transatlantic transport of black carbon-rich smoke, *Atmos. Chem. Phys.*, **20**,  
4757–4785, <https://doi.org/10.5194/acp-20-4757-2020>, 2020.
- Holanda, B.A., Franco, M.A., Walter, D., Artaxo, P., Carbone, S., Cheng, Y., Chowdhury, S., Ditas, F., Gysel-Beer, M.,  
800 Klimach, T., Krempner, L.A., Krüger, O.O., Lavric, J.V., Lelieveld, J., Ma, C., Machado, L.A.T., Modini, R.L., Morais,  
F.G., Pozzer, A., Saturno, J., Su, H., Wendisch, M., Wolff, S., Pöhlker, M.L., Andreae, M.O., Pöschl, U., & Pöhlker,  
C.: African biomass burning affects aerosol cycling over the Amazon, *Commun Earth Environ* **4**, 154,  
<https://doi.org/10.1038/s43247-023-00795-5>, 2023.
- Hughey, C. A., Hendrickson, C. L., Rodgers, R. P., Marshall, A. G., and Qian, K.: Kendrick Mass Defect Spectrum: A Compact  
805 Visual Analysis for Ultrahigh-Resolution Broadband Mass Spectra, *Anal. Chem.*, **73**, 4676–4681,  
<https://doi.org/10.1021/ac010560w>, 2001.
- Iinuma, Y., Böge, O., Gräfe, R., and Herrmann, H.: Methyl-nitrocatechols: atmospheric tracer compounds for biomass burning  
secondary organic aerosols, *Environmental science & technology*, **44**, 8453–8459,  
<https://doi.org/10.1021/es102938a>, 2010.
- 810 INPE - Instituto Nacional de Pesquisas Espaciais, 2020: Portal do Monitoramento de Queimadas e Incêndios Florestais,  
Programa Queimadas, <http://www.inpe.br/queimadas>, last access: 14 December 2020.
- Jaoui, M., Szmigielski, R., Nestorowicz, K., Kolodziejczyk, A., Sarang, K., Rudzinski, K. J., Konopka, A., Bulska, E.,  
Lewandowski, M., and Kleindienst, T. E.: Organic Hydroxy Acids as Highly Oxygenated Molecular (HOM) Tracers  
for Aged Isoprene Aerosol, *Environmental science & technology*, **53**, 14516–14527,  
815 <https://doi.org/10.1021/acs.est.9b05075>, 2019.
- Jenkin, M. E.: Modelling the formation and composition of secondary organic aerosol from  $\alpha$ - and  $\beta$ -pinene ozonolysis using  
MCM v3, *Atmos. Chem. Phys.*, **4**, 1741–1757, <https://doi.org/10.5194/acp-4-1741-2004>, 2004.
- Jimenez, J. L., Canagaratna, M. R., Donahue, N. M., Prevot, A. S. H., Zhang, Q., Kroll, J. H.,  
DeCarlo, P. F., Allan, J. D., Coe, H., Ng, N. L., Aiken, A. C., Docherty, K. S., Ulbrich, I. M., Grieshop, A. P., Robinson, A.  
820 L., Duplissy, J., Smith, J. D., Wilson, K. R., Lanz, V. A., Hueglin, C., Sun, Y. L., Tian, J., Laaksonen, A., Raatikainen,  
T., Rautiainen, J., Vaattovaara, P., Ehn, M., Kulmala, M., Tomlinson, J. M., Collins, D. R., Cubison, M. J., Dunlea,  
E. J., Huffman, J. A., Onasch, T. B., Alfarra, M. R., Williams, P. I., Bower, K., Kondo, Y., Schneider, J., Drewnick,  
F., Borrmann, S., Weimer, S., Demerjian, K., Salcedo, D., Cottrell, L., Griffin, R., Takami, A., Miyoshi, T.,  
Hatakeyama, S., Shimono, A., Sun, J. Y., Zhang, Y. M., Dzepina, K., Kimmel, J. R., Sueper, D., Jayne, J. T., Herndon,  
825 S. C., Trimborn, A. M., Williams, L. R., Wood, E. C., Middlebrook, A. M., Kolb, C. E., Baltensperger, U., and  
Worsnop, D. R.: Evolution of organic aerosols in the atmosphere, *Science (New York, N.Y.)*, **326**, 1525–1529,  
<https://doi.org/10.1126/science.1180353>, 2009.
- Joo, T., Rivera-Rios, J. C., Takeuchi, M., Alvarado, M. J., and Ng, N. L.: Secondary Organic Aerosol Formation from Reaction  
of 3-Methylfuran with Nitrate Radicals, *ACS Earth Space Chem.*, **3**, 922–934,  
830 <https://doi.org/10.1021/acsearthspacechem.9b00068>, 2019.



- Kahnt, A., Behrouzi, S., Vermeylen, R., Safi Shalamzari, M., Vercauteren, J., Roekens, E., Claeys, M., and Maenhaut, W.: One-year study of nitro-organic compounds and their relation to wood burning in PM10 aerosol from a rural site in Belgium, *Atmospheric Environment*, 81, 561–568, <https://doi.org/10.1016/j.atmosenv.2013.09.041>, 2013.
- 835 Kanakidou, M., Seinfeld, J. H., Pandis, S. N., Barnes, I., Dentener, F. J., Facchini, M. C., van Dingenen, R., Ervens, B., Nenes, A., Nielsen, C. J., Swietlicki, E., Putaud, J. P., Balkanski, Y., Fuzzi, S., Horth, J., Moortgat, G. K., Winterhalter, R., Myhre, C. E. L., Tsigaridis, K., Vignati, E., Stephanou, E. G., and Wilson, J.: Organic aerosol and global climate modelling: a review, *Atmos. Chem. Phys.*, 5, 1053–1123, <https://doi.org/10.5194/acp-5-1053-2005>, 2005.
- Kautzman, K. E., Surratt, J. D., Chan, M. N., Chan, A. W. H., Hersey, S. P., Chhabra, P. S., Dalleska, N. F., Wennberg, P. O., Flagan, R. C., and Seinfeld, J. H.: Chemical composition of gas- and aerosol-phase products from the photooxidation of naphthalene, *The journal of physical chemistry. A*, 114, 913–934, <https://doi.org/10.1021/jp908530s>, 2010.
- 840 Kendrick, E.: A Mass Scale Based on CH<sub>2</sub> = 14.0000 for High Resolution Mass Spectrometry of Organic Compounds, *Anal. Chem.*, 35, 2146–2154, <https://doi.org/10.1021/ac60206a048>, 1963.
- Kitanovski, Z., Grgić, I., Yasmeen, F., Claeys, M., and Cusak, A.: Development of a liquid chromatographic method based on ultraviolet-visible and electrospray ionization mass spectrometric detection for the identification of nitrocatechols and related tracers in biomass burning atmospheric organic aerosol, *Rapid communications in mass spectrometry RCM*, 26, 793–804, <https://doi.org/10.1002/rcm.6170>, 2012.
- 845 Kleindienst, T. E., Jaoui, M., Lewandowski, M., Offenberg, J. H., Lewis, C. W., Bhawe, P. V., and Edney, E. O.: Estimates of the contributions of biogenic and anthropogenic hydrocarbons to secondary organic aerosol at a southeastern US location, *Atmospheric Environment*, 41, 8288–8300, <https://doi.org/10.1016/j.atmosenv.2007.06.045>, 2007.
- 850 Kong, X., Salvador, C. M., Carlsson, S., Pathak, R., Davidsson, K. O., Le Breton, M., Gaita, S. M., Mitra, K., Hallquist, Å. M., Hallquist, M., and Pettersson, J. B. C.: Molecular characterization and optical properties of primary emissions from a residential wood burning boiler, *The Science of the total environment*, 754, 142143, <https://doi.org/10.1016/j.scitotenv.2020.142143>, 2021.
- 855 Kourtchev, I., Godoi, R.H.M., Connors, S., Levine, J.G., Archibald, A., Godoi, A.F.L., Paralovo, S., Barbosa, C.G.G., Souza, R.A.F., Manzi, A.O., Seco, R., Sjostedt, S., Park, J.-H., Guenther, A., Kim, S., Smith, J., Martin, S.T. and Kalberer, M.: Molecular composition of organic aerosols in central Amazonia: An ultra-high resolution mass spectrometry study, *Atmos. Chem. Phys.*, 16, 11899–11913, <https://doi.org/10.5194/acp-16-11899-2016>, 2016.
- 860 Kourtchev, I., Fuller, S. J., Giorio, C., Healy, R. M., Wilson, E., O'Konski, Connor, I., Wenger, J. C., McLeod, M., Aalto, J., Ruuskanen, T. M., Maenhaut, W., Jones, R., Venables, D. S., Sodeau, J. R., Kulmala, M., and Kalberer, M.: Molecular composition of biogenic secondary organic aerosols using ultrahigh-resolution mass spectrometry: Comparing laboratory and field studies, *Atmos. Chem. Phys.*, 14, 2155–2167, <https://doi.org/10.5194/acp-14-2155-2014>, 2014a.
- 865 Kourtchev, I., O'Connor, I. P., Giorio, C., Fuller, S. J., Kristensen, K., Maenhaut, W., Wenger, J. C., Sodeau, J. R., Glasius, M., and Kalberer, M.: Effects of anthropogenic emissions on the molecular composition of urban organic aerosols: An ultrahigh resolution mass spectrometry study, *Atmospheric Environment*, 89, 525–532, <https://doi.org/10.1016/j.atmosenv.2014.02.051>, 2014b.
- Kourtchev, I., Fuller, S., Aalto, J., Ruuskanen, T. M., McLeod, M. W., Maenhaut, W., Jones, R., Kulmala, M., and Kalberer, M.: Molecular composition of boreal forest aerosol from Hyytiälä, Finland, using ultrahigh resolution mass spectrometry, *Environmental science & technology*, 47, 4069–4079, <https://doi.org/10.1021/es3051636>, 2013.
- 870 Kourtchev, I., Sebben, B.G., Brill, S., Cybelli, G.G.B., Weber, B., Ferreira, R.R., D'Oliveira, F.A.F., Dias, C.Q. Jr., Popoola, O.A.M., Williams, J., Pöhlker, C., Godoi, R.H.M., Occurrence of a " forever chemical " in the atmosphere above pristine Amazon Forest, *Sci. Total Environ.*, 944, AR 173918, [10.1016/j.scitotenv.2024.173918](https://doi.org/10.1016/j.scitotenv.2024.173918), 2024.



- Krechmer, J. E., Coggon, M. M., Massoli, P., Nguyen, T. B., Crounse, J. D., Hu, W., Day, D. A., Tyndall, G. S., Henze, D. K., Rivera-Rios, J. C., Nowak, J. B., Kimmel, J. R., Mauldin, R. L., Stark, H., Jayne, J. T., Sipilä, M., Junninen, H., Clair, J. M. S., Zhang, X., Feiner, P. A., Zhang, L., Miller, D. O., Brune, W. H., Keutsch, F. N., Wennberg, P. O., Seinfeld, J. H., Worsnop, D. R., Jimenez, J. L., and Canagaratna, M. R.: Formation of Low Volatility Organic Compounds and Secondary Organic Aerosol from Isoprene Hydroxyhydroperoxide Low-NO Oxidation, *Environmental science & technology*, 49, 10330–10339, <https://doi.org/10.1021/acs.est.5b02031>, 2015.
- Kristensen, K., Enggrob, K. L., King, S. M., Worton, D. R., Platt, S. M., Mortensen, R., Rosenoern, T., Surratt, J. D., Bilde, M., Goldstein, A. H., and Glasius, M.: Formation and occurrence of dimer esters of pinene oxidation products in atmospheric aerosols, *Atmos. Chem. Phys.*, 13, 3763–3776, <https://doi.org/10.5194/acp-13-3763-2013>, 2013.
- Kroll, J. H. and Seinfeld, J. H.: Chemistry of secondary organic aerosol: Formation and evolution of low-volatility organics in the atmosphere, *Atmospheric Environment*, 42, 3593–3624, <https://doi.org/10.1016/j.atmosenv.2008.01.003>, 2008.
- Kroll, J. H., Donahue, N. M., Jimenez, J. L., Kessler, S. H., Canagaratna, M. R., Wilson, K. R., Altieri, K. E., Mazzoleni, L. R., Wozniak, A. S., Bluhm, H., Mysak, E. R., Smith, J. D., Kolb, C. E., and Worsnop, D. R.: Carbon oxidation state as a metric for describing the chemistry of atmospheric organic aerosol, *Nature chemistry*, 3, 133–139, <https://doi.org/10.1038/nchem.948>, 2011.
- Kundu, S., Fisseha, R., Putman, A. L., Rahn, T. A., and Mazzoleni, L. R.: High molecular weight SOA formation during limonene ozonolysis: insights from ultrahigh-resolution FT-ICR mass spectrometry characterization, *Atmos. Chem. Phys.*, 12, 5523–5536, <https://doi.org/10.5194/acp-12-5523-2012>, 2012.
- Laskin, A., Smith, J. S., and Laskin, J.: Molecular characterization of nitrogen-containing organic compounds in biomass burning aerosols using high-resolution mass spectrometry, *Environ. Sci. Technol.*, 43, 3764–3771, <https://doi.org/10.1021/es803456n>, 2009.
- Li, Y., Pöschl, U., and Shiraiwa, M.: Molecular corridors and parameterizations of volatility in the chemical evolution of organic aerosols, *Atmos. Chem. Phys.*, 16, 3327–3344, <https://doi.org/10.5194/acp-16-3327-2016>, 2016.
- Lin, P., Aiona, P. K., Li, Y., Shiraiwa, M., Laskin, J., Nizkorodov, S. A., and Laskin, A.: Molecular Characterization of Brown Carbon in Biomass Burning Aerosol Particles, *Environmental science & technology*, 50, 11815–11824, <https://doi.org/10.1021/acs.est.6b03024>, 2016.
- Lin, P., Rincon, A. G., Kalberer, M., and Yu, J. Z.: Elemental composition of HULIS in the Pearl River Delta Region, China: results inferred from positive and negative electrospray high resolution mass spectrometric data, *Environmental science & technology*, 46, 7454–7462, <https://doi.org/10.1021/es300285d>, 2012.
- Lin, P., Fleming, L. T., Nizkorodov, S. A., Laskin, J., Laskin, A.: Comprehensive Molecular Characterization of Atmospheric Brown Carbon by High Resolution Mass Spectrometry with Electrospray and Atmospheric, Pressure Photoionization, *Anal. Chem.*, 90(21), 12493–12502, <https://doi.org/10.1021/acs.analchem.8b02177>, 2018.
- Mazzoleni, L. R., Saranjampour, P., Dalbec, M. M., Samburova, V., Hallar, A. G., Zielinska, B., Lowenthal, D. H., and Kohl, S.: Identification of water-soluble organic carbon in non-urban aerosols using ultrahigh-resolution FT-ICR mass spectrometry: organic anions, *Environ. Chem.*, 9, 285, <https://doi.org/10.1071/EN11167>, 2012.
- Mettler, M. S., Mushrif, S. H., Paulsen, A. D., Javadekar, A. D., Vlachos, D. G., and Dauenhauer, P. J.: Revealing pyrolysis chemistry for biofuels production: Conversion of cellulose to furans and small oxygenates, *Energy Environ. Sci.*, 5, 5414–5424, <https://doi.org/10.1039/C1EE02743C>, 2012.
- Molteni, U., Bianchi, F., Klein, F., El Haddad, I., Frege, C., Rossi, M. J., Dommen, J., and Baltensperger, U.: Formation of highly oxygenated organic molecules from aromatic compounds, 2016.
- Monks, P. S.: Gas-phase radical chemistry in the troposphere, *Chemical Society reviews*, 34, 376–395, <https://doi.org/10.1039/b307982c>, 2005.





- Murphy, B. N., Donahue, N. M., Robinson, A. L., and Pandis, S. N.: A naming convention for atmospheric organic aerosol, *Atmos. Chem. Phys.*, 14, 5825–5839, <https://doi.org/10.5194/acp-14-5825-2014>, 2014.
- Nagori, J., Janssen, R. H. H., Fry, J. L., Krol, M., Jimenez, J. L., Hu, W., and Vilà-Guerau de Arellano, J.: Biogenic emissions and land–atmosphere interactions as drivers of the daytime evolution of secondary organic aerosol in the southeastern US, *Atmos. Chem. Phys.*, 19, 701–729, <https://doi.org/10.5194/acp-19-701-2019>, 2019.
- Nguyen, T. B., Roach, P. J., Laskin, J., Laskin, A., and Nizkorodov, S. A.: Effect of humidity on the composition of isoprene photooxidation secondary organic aerosol, *Atmos. Chem. Phys.*, 11, 6931–6944, <https://doi.org/10.5194/acp-11-6931-2011>, 2011.
- Nguyen, T. B., Bateman, A. P., Bones, D. L., Nizkorodov, S. A., Laskin, J., and Laskin, A.: High-resolution mass spectrometry analysis of secondary organic aerosol generated by ozonolysis of isoprene, *Atmospheric Environment*, 44, 1032–1042, <https://doi.org/10.1016/j.atmosenv.2009.12.019>, 2010.
- Nizkorodov, S. A., Laskin, J., and Laskin, A.: Molecular chemistry of organic aerosols through the application of high resolution mass spectrometry, *Physical chemistry chemical physics PCCP*, 13, 3612–3629, <https://doi.org/10.1039/C0CP02032J>, 2011.
- Nolte, C. G., Schauer, J. J., Cass, G. R., and Simoneit, B. R.: Highly polar organic compounds present in wood smoke and in the ambient atmosphere, *Environ. Sci. Technol.*, 35, 1912–1919, <https://doi.org/10.1021/es001420r>, 2001.
- Nozière, B., Kalberer, M., Claeys, M., Allan, J., D'Anna, B., Decesari, S., Finessi, E., Glasius, M., Grgić, I., Hamilton, J. F., Hoffmann, T., Iinuma, Y., Jaoui, M., Kahnt, A., Kampf, C. J., Kourtev, I., Maenhaut, W., Marsden, N., Saarikoski, S., Schnelle-Kreis, J., Surratt, J. D., Szidat, S., Szmigielski, R., and Wisthaler, A.: The molecular identification of organic compounds in the atmosphere: state of the art and challenges, *Chemical reviews*, 115, 3919–3983, <https://doi.org/10.1021/cr5003485>, 2015.
- Odum, J. R., Hoffmann, T., Bowman, F., Collins, D. R., Flagan, R. C., and Seinfeld, J. H.: Gas/Particle Partitioning and Secondary Organic Aerosol Yields, *Environ. Sci. Technol.*, 30, 2580–2585, <https://doi.org/10.1021/es950943+>, 1996.
- Oros, D. R. and Simoneit, B. R.: Identification and emission factors of molecular tracers in organic aerosols from biomass burning Part 1. Temperate climate conifers, *Applied Geochemistry*, 16, 1513–1544, [https://doi.org/10.1016/S0883-2927\(01\)00021-X](https://doi.org/10.1016/S0883-2927(01)00021-X), 2001.
- Pankow, J. F.: An absorption model of the gas/aerosol partitioning involved in the formation of secondary organic aerosol, *Atmospheric Environment*, 28, 189–193, [https://doi.org/10.1016/1352-2310\(94\)90094-9](https://doi.org/10.1016/1352-2310(94)90094-9), 1994.
- Paulot, F., Crounse, J. D., Kjaergaard, H. G., Kurten, A., St Clair, J. M., Seinfeld, J. H., and Wennberg, P. O.: Unexpected epoxide formation in the gas-phase photooxidation of isoprene, *Science (New York, N.Y.)*, 325, 730–733, <https://doi.org/10.1126/science.1172910>, 2009.
- Peeters, J., Vereecken, L., and Fantechi, G.: The detailed mechanism of the OH-initiated atmospheric oxidation of  $\alpha$ -pinene: a theoretical, *Physical chemistry chemical physics PCCP*, 3, 5489–5504, <https://doi.org/10.1039/b106555f>, 2001.
- Pöhlker, M. L., Pöhlker, C., Quaas, J. et al. Global organic and inorganic aerosol hygroscopicity and its effect on radiative forcing, *Nat Commun* 14, 6139, <https://doi.org/10.1038/s41467-023-41695-8>, 2023.
- Pöhlker, M. L., Ditas, F., Saturno, J., Klimach, T., Hrabě de Angelis, I., Araújo, A. C., Brito, J., Carbone, S., Cheng, Y., Chi, X., Ditz, R., Gunthe, S. S., Holanda, B. A., Kandler, K., Kesselmeier, J., Könemann, T., Krüger, O. O., Lavrič, J. V., Martin, S. T., Mikhailov, E., Moran-Zuloaga, D., Rizzo, L. V., Rose, D., Su, H., Thalman, R., Walter, D., Wang, J., Wolff, S., Barbosa, H. M. J., Artaxo, P., Andreae, M. O., Pöschl, U., and Pöhlker, C.: Long-term observations of cloud condensation nuclei over the Amazon rain forest – Part 2: Variability and characteristics of biomass burning, long-range transport, and pristine rain forest aerosols, *Atmos. Chem. Phys.*, 18, 10289–10331, <https://doi.org/10.5194/acp-18-10289-2018>, 2018.





- Pöhlker, C., Walter, D., Paulsen, H., Könemann, T., Rodríguez-Caballero, E., Moran-Zuloaga, D., Brito, J., Carbone, S., Degrendele, C., Després, V. R., Ditas, F., Holanda, B. A., Kaiser, J. W., Lammel, G., Lavrič, J. V., Ming, J., Pickersgill, D., Pöhlker, M. L., Praß, M., Löbs, N., Saturno, J., Sörgel, M., Wang, Q., Weber, B., Wolff, S., Artaxo, P., Pöschl, U., and Andreae, M. O.: Land cover and its transformation in the backward trajectory footprint region of the Amazon Tall Tower Observatory, *Atmos. Chem. Phys.*, 19, 8425–8470, <https://doi.org/10.5194/acp-19-8425-2019>, 2019.
- Pöschl, U., Martin, S. T., Sinha, B., Chen, Q., Gunthe, S. S., Huffman, J. A., Borrmann, S., Farmer, D. K., Garland, R. M., Helas, G., Jimenez, J. L., King, S. M., Manzi, A., Mikhailov, E., Pauliquevis, T., Petters, M. D., Prenni, A. J., Roldin, P., Rose, D., Schneider, J., Su, H., Zorn, S. R., Artaxo, P., and Andreae, M. O.: Rainforest aerosols as biogenic nuclei of clouds and precipitation in the Amazon, *Science* (New York, N.Y.), 329, 1513–1516, <https://doi.org/10.1126/science.1191056>, 2010.
- Pöschl, U.: Atmospheric aerosols: composition, transformation, climate and health effects, *Angewandte Chemie (International ed. in English)*, 44, 7520–7540, <https://doi.org/10.1002/anie.200501122>, 2005.
- Pugliese, G., Ingrisch, J., Meredith, L.K. et al. Effects of drought and recovery on soil volatile organic compound fluxes in an experimental rainforest. *Nat Commun* 14, 5064, <https://doi.org/10.1038/s41467-023-40661-8>, 2023.
- Putman, A. L., Offenberg, J. H., Fisseha, R., Kundu, S., Rahn, T. A., and Mazzoleni, L. R.: Ultrahigh-resolution FT-ICR mass spectrometry characterization of  $\alpha$ -pinene ozonolysis SOA, *Atmospheric Environment*, 46, 164–172, <https://doi.org/10.1016/j.atmosenv.2011.10.003>, 2012.
- Reinhardt, A., Emmenegger, C., Gerrits, B., Panse, C., Dommen, J., Baltensperger, U., Zenobi, R., and Kalberer, M.: Ultrahigh mass resolution and accurate mass measurements as a tool to characterize oligomers in secondary organic aerosols, *Anal. Chem.*, 79, 4074–4082, <https://doi.org/10.1021/ac062425v>, 2007.
- Rincón, A. G., Calvo, A. I., Dietzel, M., and Kalberer, M.: Seasonal differences of urban organic aerosol composition – an ultra-high resolution mass spectrometry study, *Environ. Chem.*, 9, 298, <https://doi.org/10.1071/EN12016>, 2012.
- Rolph, G., Stein, A., and Stunder, B.: Real-time Environmental Applications and Display sYstem: READY, *Environmental Modelling & Software*, 95, 210–228, <https://doi.org/10.1016/j.envsoft.2017.06.025>, 2017.
- Samburova, V., Connolly, J., Gyawali, M., Yatavelli, R. L. N., Watts, A. C., Chakrabarty, R. K., Zielinska, B., Moosmüller, H., and Khlystov, A.: Polycyclic aromatic hydrocarbons in biomass-burning emissions and their contribution to light absorption and aerosol toxicity, *The Science of the total environment*, 568, 391–401, <https://doi.org/10.1016/j.scitotenv.2016.06.026>, 2016.
- Schauer, J. J., Kleeman, M. J., Cass, G. R., and Simoneit, B. R.: Measurement of emissions from air pollution sources. 3. C1–C29 organic compounds from fireplace combustion of wood, *Environ. Sci. Technol.*, 35, 1716–1728, <https://doi.org/10.1021/es001331e>, 2001.
- Seinfeld, J. H. and Pandis, S. N.: *Atmospheric Chemistry and Physics: From Air Pollution to Climate Change*, 3r, John Wiley & Sons, 944 s, 2016.
- Seinfeld, J. H. and Pankow, J. F.: Organic atmospheric particulate material, *Annual review of physical chemistry*, 54, 121–140, <https://doi.org/10.1146/annurev.physchem.54.011002.103756>, 2003.
- Shiraiwa, M., Berkemeier, T., Schilling-Fahnestock, K. A., Seinfeld, J. H., and Pöschl, U.: Molecular corridors and kinetic regimes in the multiphase chemical evolution of secondary organic aerosol, *Atmos. Chem. Phys.*, 14, 8323–8341, <https://doi.org/10.5194/acp-14-8323-2014>, 2014.
- Shrivastava, M., Andreae, M.O., Artaxo, P., Barbosa, H.M., Berg, L.K., Brito, J., Ching, J., Easter, R.C., Fan, J., Fast, J.D. and Feng, Z.: Urban pollution greatly enhances formation of natural aerosols over the Amazon rainforest, *Nature Communications*, 10, <https://doi.org/10.1038/s41467-019-08909-4>, 2019.



- 1000 Siemens, K.S.A., Pagonis, D., Guo, H.Y., Schueneman, M.K., Dibb, J.E., Campuzano-Jost, P., Jimenez, J.L. and Laskin, A. :  
Probing Atmospheric Aerosols by Multimodal Mass Spectrometry Techniques: Revealing Aging Characteristics of  
Its Individual Molecular Components, *ACS Earth Space Chem.* 7(12), 2498-2510, <https://doi.org/10.1021/acsearthspacechem.3c00228>, 2023.
- Simoneit, B.R.T., Schauer, J. J., Nolte, C. G., Oros, D. R., Elias, V. O., Fraser, M. P., Rogge, W. F., and Cass, G. R.:  
1005 Levoglucosan, a tracer for cellulose in biomass burning and atmospheric particles, *Atmospheric Environment*, 33,  
173–182, [https://doi.org/10.1016/S1352-2310\(98\)00145-9](https://doi.org/10.1016/S1352-2310(98)00145-9), 1999.
- Stein, A. F., Draxler, R. R., Rolph, G. D., Stunder, B. J. B., Cohen, M. D., and Ngan, F.: NOAA's HYSPLIT Atmospheric  
Transport and Dispersion Modeling System, *Bulletin of the American Meteorological Society*, 96, 2059–2077,  
<https://doi.org/10.1175/BAMS-D-14-00110.1>, 2015.
- 1010 Stephanou, E. G. and Stratigakis, N.: Oxocarboxylic and .alpha.,.omega.-dicarboxylic acids: photooxidation products of  
biogenic unsaturated fatty acids present in urban aerosols, *Environ. Sci. Technol.*, 27, 1403–1407,  
<https://doi.org/10.1021/es00044a016>, 1993.
- Surratt, J. D., Gómez-González, Y., Chan, A. W. H., Vermeylen, R., Shahgholi, M., Kleindienst, T. E., Edney, E. O.,  
Offenberg, J. H., Lewandowski, M., Jaoui, M., Maenhaut, W., Claeys, M., Flagan, R. C., and Seinfeld, J. H.:  
1015 Organosulfate formation in biogenic secondary organic aerosol, *The journal of physical chemistry. A*, 112, 8345–  
8378, <https://doi.org/10.1021/jp802310p>, 2008.
- Surratt, J. D., Kroll, J. H., Kleindienst, T. E., Edney, E. O., Claeys, M., Sorooshian, A., Ng, N. L., Offenberg, J. H.,  
Lewandowski, M., Jaoui, M., Flagan, R. C., and Seinfeld, J. H.: Evidence for Organosulfates in Secondary Organic  
Aerosol, *Environ. Sci. Technol.*, 41, 517–527, <https://doi.org/10.1021/es062081q>, 2007.
- 1020 Szmigielski, R., Surratt, J. D., Gómez-González, Y., van der Veken, P., Kourtchev, I., Vermeylen, R., Blockhuys, F., Jaoui,  
M., Kleindienst, T. E., Lewandowski, M., Offenberg, J. H., Edney, E. O., Seinfeld, J. H., Maenhaut, W., and Claeys,  
M.: 3-methyl-1,2,3-butanetricarboxylic acid: An atmospheric tracer for terpene secondary organic aerosol, *Geophys.*  
*Res. Lett.*, 34, D16312, <https://doi.org/10.1029/2007GL031338>, 2007.
- Tervahattu, H., Juhanaja, J., and Kupiainen, K.: Identification of an organic coating on marine aerosol particles by TOF-SIMS,  
1025 *J. Geophys. Res.*, 107, <https://doi.org/10.1029/2001JD001403>, 2002.
- Thoma, M., Bachmeier, F., Gottwald, F.L., Simon, M., Vogel, A.L.: Mass spectrometry-based Aerosolomics: A new approach  
to resolve sources, composition, and partitioning of secondary organic aerosol, *Atmos. Meas. Techn.* 15(23), 7137–  
7154, <https://doi.org/10.5194/amt-15-7137-2022>, 2022.
- Tolocka, M. P., Jang, M., Ginter, J. M., Cox, F. J., Kamens, R. M., and Johnston, M. V.: Formation of Oligomers in Secondary  
1030 Organic Aerosol, *Environ. Sci. Technol.*, 38, 1428–1434, <https://doi.org/10.1021/es035030r>, 2004.
- Tong, H., Kourtchev, I., Pant, P., Keyte, I. J., O'Connor, I. P., Wenger, J. C., Pope, F. D., Harrison, R. M., and Kalberer, M.:  
Molecular composition of organic aerosols at urban background and road tunnel sites using ultra-high resolution mass  
spectrometry, *Faraday Discuss.*, 189, 51–68, <https://doi.org/10.1039/c5fd00206k>, 2016.
- Tu, P., Hall, W. A., and Johnston, M. V.: Characterization of Highly Oxidized Molecules in Fresh and Aged Biogenic  
1035 Secondary Organic Aerosol, *Analytical chemistry*, 88, 4495–4501, <https://doi.org/10.1021/acs.analchem.6b00378>,  
2016.
- Wang, X., Hayeck, N., Brüggemann, M., Yao, L., Chen, H., Zhang, C., Emmelin, C., Chen, J., George, C., and Wang, L.:  
Chemical Characteristics of Organic Aerosols in Shanghai: A Study by Ultrahigh-Performance Liquid  
Chromatography Coupled With Orbitrap Mass Spectrometry, *J. Geophys. Res.*, 122, 11,703–11,722,  
1040 <https://doi.org/10.1002/2017JD026930>, 2017.
- Worton, D. R., Surratt, J. D., Lafranchi, B. W., Chan, A. W. H., Zhao, Y., Weber, R. J., Park, J.-H., Gilman, J. B., Gouw, J.  
de, Park, C., Schade, G., Beaver, M., Clair, J. M. S., Crounse, J., Wennberg, P., Wolfe, G. M., Harrold, S., Thornton,



- 1045 J. A., Farmer, D. K., Docherty, K. S., Cubison, M. J., Jimenez, J.-L., Frossard, A. A., Russell, L. M., Kristensen, K., Glasius, M., Mao, J., Ren, X., Brune, W., Browne, E. C., Pusede, S. E., Cohen, R. C., Seinfeld, J. H., and Goldstein, A. H.: Observational insights into aerosol formation from isoprene, *Environmental science & technology*, 47, 11403–11413, <https://doi.org/10.1021/es4011064>, 2013.
- Wozniak, A. S., Bauer, J. E., Sleighter, R. L., Dickhut, R. M., and Hatcher, P. G.: Technical Note: Molecular characterization of aerosol-derived water soluble organic carbon using ultrahigh resolution electrospray ionization Fourier transform ion cyclotron resonance mass spectrometry, *Atmos. Chem. Phys.*, 8, 5099–5111, <https://doi.org/10.5194/acp-8-5099-2008>, 2008.
- 1050 Xie, Q.R. and Laskin, A.: Molecular characterization of atmospheric organic aerosols: Contemporary applications of high-resolution mass spectrometry, *TrAC, Trends Anal. Chem.* 181. <https://doi.org/10.1016/j.trac.2024.117986>, 2024.
- Yáñez-Serrano, A. M., Nölscher, A. C., Bourtsoukidis, E., Gomes Alves, E., Ganzeveld, L., Bonn, B., Wolff, S., Sa, M., Yamasoe, M., Williams, J., Andreae, M. O., and Kesselmeier, J.: Monoterpene chemical speciation in a tropical rainforest: variation with season, height, and time of day at the Amazon Tall Tower Observatory (ATTO), *Atmos. Chem. Phys.*, 18, 3403–3418, <https://doi.org/10.5194/acp-18-3403-2018>, 2018.
- 1055 Yassine, M. M., Harir, M., Dabek-Zlotorzynska, E., and Schmitt-Kopplin, P.: Structural characterization of organic aerosol using Fourier transform ion cyclotron resonance mass spectrometry: aromaticity equivalent approach, *Rapid communications in mass spectrometry RCM*, 28, 2445–2454, <https://doi.org/10.1002/rcm.7038>, 2014.
- 1060 Zannoni, N., Leppla, D., Lembo Silveira de Assis, P.I. et al. Surprising chiral composition changes over the Amazon rainforest with height, time and season. *Commun Earth Environ* 1, 4. <https://doi.org/10.1038/s43247-020-0007-9>, 2020.
- Zhang, Q., Jimenez, J. L., Canagaratna, M. R., Allan, J. D., Coe, H., Ulbrich, I., Alfarra, M. R., Takami, A., Middlebrook, A. M., Sun, Y. L., Dzepina, K., Dunlea, E., Docherty, K., DeCarlo, P. F., Salcedo, D., Onasch, T., Jayne, J. T., Miyoshi, T., Shimojo, A., Hatakeyama, S., Takegawa, N., Kondo, Y., Schneider, J., Drewnick, F., Borrmann, S., Weimer, S., Demerjian, K., Williams, P., Bower, K., Bahreini, R., Cottrell, L., Griffin, R. J., Rautiainen, J., Sun, J. Y., Zhang, Y. M., and Worsnop, D. R.: Ubiquity and dominance of oxygenated species in organic aerosols in anthropogenically-influenced Northern Hemisphere midlatitudes, *Geophys. Res. Lett.*, 34, n/a-n/a, <https://doi.org/10.1029/2007GL029979>, 2007.
- 1065 Zhang, Y. Y., Müller, L., Winterhalter, R., Moortgat, G. K., Hoffmann, T., and Pöschl, U.: Seasonal cycle and temperature dependence of pinene oxidation products, dicarboxylic acids and nitrophenols in fine and coarse air particulate matter, *Atmos. Chem. Phys.*, 10, 7859–7873, <https://doi.org/10.5194/acp-10-7859-2010>, 2010.
- Zhang Y, Wang K, Tong H, Huang RJ, Hoffmann T.: The maximum carbonyl ratio (MCR) as a new index for the structural classification of secondary organic aerosol components. *Rapid Commun Mass Spectrom*, 35(14):e9113. doi: 10.1002/rcm.9113, 2021.